Scaling of the reinforcement of soil slopes by living plants in a geotechnical centrifuge

Liang, Teng; Bengough, Anthony; Knappett, Jonathan; Muir Wood, David; Loades, Kenneth W.; Hallett, Paul D.; Boldrin, David; Leung, Anthony; Meijer, Gerrit

Published in:
Ecological Engineering

DOI:
10.1016/j.ecoleng.2017.06.067

Publication date:
2017

Document Version
Version created as part of publication process; publisher's layout; not normally made publicly available

Ecological Engineering xxx (2017) xxx–xxx

Contents lists available at ScienceDirect

Ecological Engineering

journal homepage: www.elsevier.com/locate/ecoleng

Scaling of the reinforcement of soil slopes by living plants in a geotechnical centrifuge

T. Liang[a,*], A.G. Bengough[a,b], J.A. Knappett[a], D. MuirWood[a], K.W. Loades[b], P.D. Hallett[c], D. Boldrin[a], A.K. Leung[a], G.J. Meijer[a]

[a] School of Science and Engineering, University of Dundee, Dundee DD1 4HN, UK
[b] James Hutton Institute, Invergowrie, Dundee DD2 5DA, UK
[c] School of Biological Sciences, University of Aberdeen, Aberdeen AB24 3UU, UK

ARTICLE INFO

Article history:
Received 17 January 2017
Received in revised form 26 June 2017
Accepted 30 June 2017
Available online xxx

Keywords:
Ecological engineering
Bioengineering
Vegetation
Slopes
Centrifuge modelling
Root reinforcement

ABSTRACT

Understanding root-reinforcement of vegetated slopes is hindered by the cost and practicality of full scale tests to explore global behaviour at the slope scale, and the idealised nature of smaller-scale testing to date that has relied on model root analogues. In this study we investigated the potential to use living plant roots in small scale experiments of slope failure that would use a geotechnical centrifuge to achieve soil stress states comparable to those in the field at homologous points. Three species (Willow, Gorse and Festulolium grass), corresponding to distinct plant groups with different root architecture and 'woodiness' were selected and cultivated for short periods (2 months for Willow and Festulolium grass, 3 months for Gorse). The morphologies, tensile strength and Young's modulus of these juvenile root samples and their effects on increasing soil shear strength were then measured (via tensile tests and direct shear tests) and compared with published results of more mature field grown specimens. Our test results show that when all juvenile root samples of the three species are considered, the commonly used negative power law does not fit the data for the relationship between root tensile strength and root diameter well, resulting in very low R^2 values ($R^2 < 0.14$). No significant differences in tensile strength were observed between roots with different diameter for Willow and Gorse, and the average root tensile strength for all juvenile root samples was 8.70 ± 0.60 MPa (Mean $\pm$ SE), 9.50 ± 0.40 MPa, 21.67 ± 1.29 MPa for Willow, Festulolium grass and Gorse, respectively. However, a strong linear relationship was observed between tensile strength and Young's modulus of the roots of the juvenile plants ($R^2 = 0.55$, 0.69, 0.50 for Willow, Festulolium grass and Gorse, respectively). From a centrifuge modelling perspective, it was shown that using juvenile plants could potentially produce prototype root systems that are highly representative of corresponding mature root systems both in terms of root mechanical properties and root morphology when a suitable growing time (2 months) and scaling factor ($N = 15$) are selected. However, it remains a challenge to simultaneously simulate the distribution of root biomass with depth of the corresponding mature plant. Therefore, a compromise has to made to resolve the conflicts between the scaling of rooting depth and root reinforcement, and it is suggested that 1:15 scale would represent a suitable compromise for studying slope failure in a geotechnical centrifuge.

1. Introduction

Vegetation as an effective and environmental-friendly approach to improve slope stability has been recognised in geotechnical and ecological engineering practice to prevent shallow landslides and erosion. Planting trees, shrubs or grasses on slopes not only improves aesthetic appearance, but more importantly: (i) controls the groundwater regime and slope hydrology (e.g. Smethurst et al., 2006, 2012, 2015) and (ii) directly increases shear strength as roots act like miniature anchors/piles for soil reinforcement (Stokes et al., 2009; Schwarz et al., 2010b). The approach can be more cost-effective than traditional engineering approaches of soil nails or micropiles, but uncertainty that remains about the effects of roots on slope stabilisation hinders uptake of the use of vegetation to stabilise slopes by practitioners (Stokes et al., 2014; Kim et al., 2017). To quantify the mechanical effect of roots on soil shear strength, many studies have been performed either in the laboratory (Waldron, 1977; Operstein and Frydman, 2000; Normaniza et al., 2008; Mickovski et al., 2009; Loades et al., 2010; Veylon et al., 2015) or the field (Hengchaovanich and Nilaweera, 1996; Wu

* Corresponding author.
E-mail address: tzliang@dundee.ac.uk (T. Liang).

http://dx.doi.org/10.1016/j.ecoleng.2017.06.067

and Watson, 1998; Ekanayake et al., 1998; Van Beek et al., 2005; Cammeraat et al., 2005; Docker and Hubble, 2008; Fan and Su, 2008; Fan and Chen, 2010; Comino and Druetta, 2010; Comino et al., 2010) using direct shear tests. However, most of these existing studies focus on the strength of soil reinforced by young trees and herbaceous plants. While this is important for understanding short-term improvement in stability of slopes planted with trees, only a few studies report the contribution of roots of well-developed mature trees to soil strength (important for long-term stability assessment), predominantly because of the large size of mature tree root systems and the limited size of available field shearing apparatus (Sonnenberg et al., 2011). Field monitoring of full-scale slopes could provide invaluable data on real slope behaviour. However, implementing a field trial is usually expensive, time consuming and it is often difficult to trigger a failure to identify the failure mechanism for safety reasons. Geotechnical centrifuge modelling, on the contrary, can provide a good balance between keeping expense low while maintaining a high level of fidelity and is potentially therefore a better method for investigating the global performance of vegetated slopes under known boundary conditions (Sonnenberg et al., 2010; Liang et al., 2015).

In previous applications of centrifuge modelling to study vegetated slopes, plant roots have been modelled either using root analogues (e.g. Sonnenberg et al., 2011; Eab et al., 2014; Liang et al., 2015; Ng et al., 2014, 2016) or live plants (e.g. Sonnenberg et al., 2010; Askarinejad and Springman, 2015). Root analogues have a major advantage of high repeatability of architecture and properties and they can be easily and quickly produced. The major difficulty of this modelling technique, however, is to identify a suitable material which can simultaneously model the stiffness, strength and complex architecture of live roots, though some progress has recently been made by Liang et al. (2014, 2017) and Liang and Knappett (2017), who employed the 3-D printing technique using Acrylonitrile butadiene styrene (ABS) plastic to produce root analogues of complex geometry, while simulating strength (T_r) and stiffness (E) much more realistically than previously used materials (e.g. wood or rubber dowels). However, these are limited to use in dry cohesionless soils due to the necessity of pluviating the soil around the analogues for installation.

Use of live plants in the centrifuge can potentially model both mechanical and hydrological effects. Compared to root analogues, live plants could provide not only representative root strength and stiffness, but also more correct stress-strain response, including the maximum strain and stress localisation, and highly representative root-soil interaction properties (Hinsinger et al., 2009). However, previous studies using live plants (e.g. Sonnenberg et al., 2010; Askarinejad and Springman, 2015) did not consider in detail the scaling of the properties in the model. For example, for the 290-day-old Willow used by Sonnenberg et al. (2010), tensile strength of root sample with a diameter of 0.2 mm is approximately 80 MPa at model scale. If this root is being tested in a centrifuge at a gravitational acceleration of 15g (i.e., $N = 15$), according to the centrifuge scaling laws, the root diameter at prototype scale would be 3 mm, where the root tensile strength of Willow in the field is less than 20 MPa for roots larger than 3 mm (Mickovski et al., 2009). Such over-representation of root strength could lead to over-prediction of root reinforcement and its contribution to slope stability.

Previous studies on root biomechanical properties have revealed that root tensile strength and stiffness often decrease with increasing root diameter for mature plants (e.g. Bischetti et al., 2005; Genet et al., 2005; Pollen and Simon, 2005; Zhang et al., 2014), and also that they increase with root age (Loades et al., 2015; Sonnenberg et al., 2010). Due to the counteracting effects between root diameter and root age on the root biomechanical properties, it might be possible to use juvenile fine roots to simulate the biomechanical behaviour of mature coarse roots of the same species (for similar root architecture) in centrifuge models. Docker and Hubble (2009) have previously applied a similar concept to simulate the root system architecture of mature trees using field excavated juvenile trees to study the role of mature trees on slope stability at field scale.

Table 1
Scaling laws for centrifuge testing related to this study (After Schofield, 1981; Taylor, 2003; Muir Wood, 2003).

Parameter	Scaling law: Model/Prototype	Dimensions[a]
Length/Depth	1/N	L
Area	$1/N^2$	L^2
Volume	$1/N^3$	L^3
Seepage (Consolidation Time)	$1/N^2$	T
Density	1	M/L^3
Mass	$1/N^3$	M
Stress/Tensile Strength	1	M/LT^2
Strain	1	–
Force	$1/N^2$	ML/T^2
Bending moment	$1/N^3$	ML^2/T^2
Young's modulus	1	M/LT^2
Second moment of area	$1/N^4$	L^4

[a] L = length; M = mass; T = time.

The aim of this paper is to identify candidate species to better represent scale root morphologies and mechanical characteristics for use in centrifuge modelling. After preliminary assessment of suitable species, three species, which represent three distinct plant functional groups, were selected and cultivated for limited periods of time. A series of direct shear and axial tensile tests were undertaken to quantify root morphologies, tensile strength and Young's modulus of these juvenile root samples and their effects on increased soil strength. Based on the test results, the potential uses of the juvenile root systems to model biomechanical behaviour of mature coarse roots in centrifuge were discussed through a comparison with published results of more mature field grown specimens.

2. Materials and methods

2.1. Principles of centrifuge modelling

A geotechnical centrifuge is a device which can provide an enhanced gravity field to a reduced-scale physical model via centripetal acceleration. When testing a small scale model in a geotechnical centrifuge, similitude of stresses (and therefore the non-linear stress-strain behaviour of soil) at homologous points within the model and full-scale prototype can be achieved. In this way, the global performance of a full-scale soil slope prototype can be simulated to a high level of fidelity at a small scale model. Relevant scaling laws for centrifuge modelling used in this study are show in Table 1 (Schofield, 1981; Taylor, 2003; Muir Wood, 2003). These are principally based on the concept that the model is scaled purely geometrically, with model material properties (e.g. T_r, E) scaled 1:1.

2.2. Soil properties

All plant specimens were grown in 150 mm diameter tubes 530 mm long packed with mechanically compacted Bullionfield soil (mineral portions consisting of 71% sand, 19% silt, and 10% clay, James Hutton Institute, Dundee, UK) with a pH of 6.2 (Loades et al., 2015). The length/height of the tubes was selected to be the same as the maximum depth of soil that could be modelled in a centrifuge strong-box at the University of Dundee, UK. The liquid limit and plastic limit of the soil were determined to be 0.297 gg^{-1} and 0.192 gg^{-1}, respectively, following the fall-cone test and moulding tests, described by the British Standard (BS1377:1990 Part 1). The base of each tube was covered with a mesh membrane (1 mm

Please cite this article in press as: Liang, T., et al., Scaling of the reinforcement of soil slopes by living plants in a geotechnical centrifuge. Ecol. Eng. (2017), http://dx.doi.org/10.1016/j.ecoleng.2017.06.067

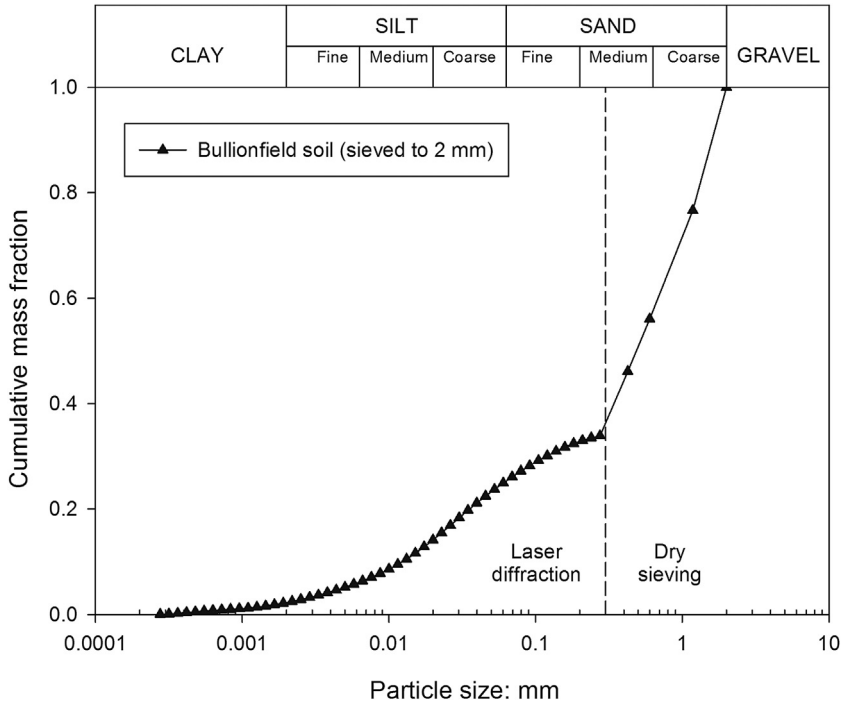

Fig. 1. Particle size distributions of Bullionfield soil sieved to 2 mm (Laser diffraction was used to quantify the amount of particles smaller than 0.3 mm, while dry sieving was adopted for particles >0.3 mm).

aperture) and an overlying thin layer of pea gravel, 20 mm thick, to facilitate drainage. Before compaction, the soil was sieved to a largest particle size of 2 mm. The soil particle size distribution (PSD) curve was determined using a combination of dry sieving (particles > 0.3 mm) and laser diffraction (particles < 0.3 mm) (BS1377:1990 Part 1) and is shown in Fig. 1. De-aired distilled water was then added to the sieved soil and mixed thoroughly to achieve a water content of 0.18 gg^{-1}, which was the optimum water content of the sieved soil samples, according to the measured relationship between dry density and water content (BS1377:1990 Part 4). The mixed sample was stored in a sealed container for a minimum period of 24 h to allow for moisture equalisation. In each tube, the soil column was packed in 10 layers using a standard 2.5 kg rammer used in the standard Procter compaction test, targeting a 1.4 g/cm^3 dry bulk density. At this density the soil has a penetration resistance of 1.22 ± 0.07 MPa, which was determined using a 2.96 mm diameter penetrometer with a 30° cone tip. If the penetrometer resistance is higher than 2 MPa, the soil will strongly impede root elongation, hence the soil samples as packed are favourable for plant growth (Schmidt et al., 2013; Bengough et al., 2016). The friction angle and cohesion of the soil at the target dry bulk density were determined to be 36.4° and 3.5 kPa, respectively, following a series of conventional direct shear tests performed on fully saturated soil samples (BS1377:1990 Part 7, 8). For each layer, 8 blows were applied, to represent an equivalent compaction energy of 67.9 kJ/m^3. During packing, a plate with a thin outer ring protruding from its surface was put on the soil surface (Mickovski et al., 2009). Hence, soil just within the rim of the tube would be compacted more and the denser soil here would discourage unwanted preferential root growth along the container walls. Soil surfaces between each successive layer were roughened prior to packing the subsequent layer to ensure full adhesion between soil layers (see Loades et al., 2013). To check the influence of potential over compaction on the bottom layer, one compacted soil core was cut into 5 segments with identical height (100 mm) and each weighed. There was no significant difference in wet density between the top and bottom layers (P > 0.5). The saturated hydraulic conductivity of the compacted soil sample is $2.15 \pm 0.15 \times 10^{-7}$ m/s, according to constant head permeability tests conducted on three 450 mm height soil cores compacted in 50 mm diameter tubes.

The soil water retention curve (SWRC) was determined using five samples packed in 100 cm^3 steel rings (average dry bulk density ρ_d = 1.42 g/cm^3). Each ring was subjected to suctions ranging from 1 to 1500 kPa using a tension table (1–50 kPa) and a pressure plate apparatus (50–1500 kPa; ELE International, Hemel Hempstead, UK). The SWRC was fitted to the Van Genuchten model (van Genuchten, 1980) in terms of gravimetric water contents:

$$w = w_r + \frac{w_s - w_r}{\left[1 + |\alpha\psi|^n\right]^m} \quad (1)$$

Where w is the soil water content (gg^{-1}), w_r is the residual soil water content at 1500 kPa (0.122 gg^{-1}), w_s is the saturated soil water content, taken as the recorded water content at the suction of 0.5 kPa (0.27 gg^{-1}), ψ is soil matric suction (kPa), and α, n and m are model parameters, fitted as 0.15 kPa^{-1}, 1.43 and $(1 - 1/n)$, respectively (R^2 = 0.98).

2.3. Plants

Three species, *Salix viminalis* (Willow, variety Tora), *Ulex europaeus* L. (Gorse) and *Lolium perenne* × *Festuca pratensis* hybrid (Festulolium grass), corresponding to distinct plant functional groups with contrasting root systems, were selected and cultivated for approximately two or three months (two month for Willow and Festulolium grass, three months for Gorse) following a preliminary assessment of suitable species for use in slope engineering applications. *Salix viminalis tora* (Willow) is a fast-growing species, and willows are widely used by ecological and geotechnical engineers as "live poles" (cuttings) to improve the stability of slopes within the UK and across the world (Mickovski et al., 2009; Wu et al., 2014). Festulolium hybrid (*L. perenne* × *F. pratensis*) was developed by the Welsh Plant Breeding Station in the 1970s, which has a typical fibrous root system and has been proposed for potential use due to its water storage/flood mitigation qualities identified in the

Please cite this article in press as: Liang, T., et al., Scaling of the reinforcement of soil slopes by living plants in a geotechnical centrifuge. Ecol. Eng. (2017), http://dx.doi.org/10.1016/j.ecoleng.2017.06.067

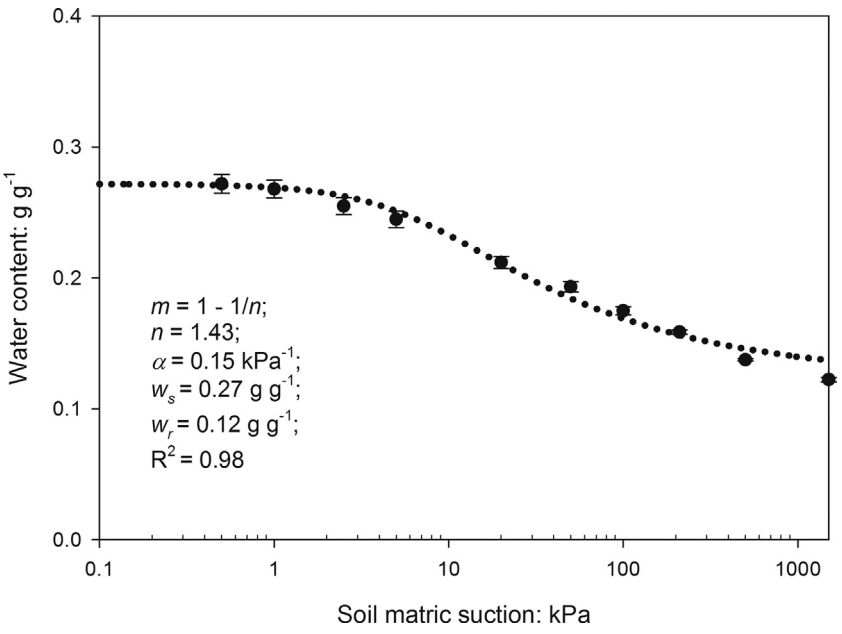

Fig. 2. Soil water retention curve of Bullionfield soil sieved to 2 mm and compacted to dry density of 1.4 g/cm^3, mean values of five replicates (±SE) are used in curve fitting for the van Genuchten (1980) model.

SuperGraSS project (Macleod et al., 2013). *Ulex europaeus* L. (Gorse) can develop a typical tap root system consisting of a thicker tap root and numerous very fine roots, which represents a very distinct root morphology compared with Willow poles and Festulolium grass. Gorse has also been shown to have high water-removing ability (resulting in improved hydrological reinforcement) compared to other tested native species in the UK according to a recent study (Boldrin et al., 2017a). For each species, 6 replicates were prepared, three of which were used for measurement of root architecture and provision of specimens for root tensile testing, while the other three were used for direct shear tests. A further three replicate pots were packed only with soil to the same density and were used as fallow controls in the shear testing programme.

2.4. Test setup

The tubes that were used for shear testing were each pre-cut at shear plane depths of 100, 200, 300 and 400 mm from the column surface to create multiple sections. To prevent interlocking between these cut surfaces during shear testing, narrow gaps between the plastic pipe sections were left deliberately by inserting 3 mm thick spacers between the two sections of each pipe, and then wrapping across the joins using a strong waterproof adhesive tape to secure the two sections together during plant growth.

For Willow cores, one 100 mm-long Willow stem cutting was inserted into each core leaving 30 mm (i.e., approximately 1/3 of the total length) protruding from the soil surface. For Gorse and grass cores, seeds were pregerminated on filter paper at 20 °C, and then healthy seedlings were transplanted when roots were 5–10 mm-long, to (aim to) achieve nine grass seedlings per core and five gorse seedlings (after initial thinning).

All tubes were placed in a designed indoor growing area at the University of Dundee, and they were left there for 60 or 90 days under controlled lighting and temperature. A standard data logger EL-USB-2 (LASCAR electronics, UK) and a Maxiswitch Pro light controller MBMSP6 (MAXIGROW LTD, UK) were used to measure and control the environmental conditions, consisting 16 h daylight per day (24 h) under controlled temperature of 27 ± 0.38 °C (Mean ± SE), and 8 h night per day at a temperature of 22 ± 0.13 °C. The recorded daily relative humidity was 41 ± 0.06%. Lights were provided by Maxibright T5 fluorescent lighting unit MBT5LW8T1-9 (MAXIGROW LTD, UK), which was equipped with eight blue T5 fluorescent tubes. Each tube could deliver 4450 lumens of light with a very low heat output. The height of lighting unit was adjusted with the growth of the plants and kept a constant distance (150 mm) away from the tallest shoot tips. Water was supplied to planted and fallow containers using a watering can every two days. Water was added regularly to maintain the soil columns at constant mass, corresponding approximately to soil field capacity (5 kPa suction, 0.25 gg^{-1}, see Fig. 2 and (Boldrin et al., 2017b)).

2.5. Root system architecture measurement

After cultivation, the nine planted samples prepared for tensile testing were carefully removed from the soil and washed, with extra care taken to not discard finer root material. The root samples were then cut into four sections corresponding to depths 150, 300 and 450 mm. Root segments below 450 mm were discarded because any roots in this region were located close to the gravel layer, where different root properties might have developed. Approximately 15% of each segment (by dry weight) was selected randomly and treated with 75% v/v alcohol for root system measurement. The remaining 85% of the samples were kept fresh for tensile tests, which were performed within 72 h after sampling. Both treated and fresh samples were labelled and stored at 4 °C on moist blotting paper. When the tensile tests were completed, roots were placed in paper bags and left to dry at 70 °C for 48 h in an oven. The total dry root biomass was then measured. Each treated sample was scanned on an A3 size flat-bed scanner at a resolution of 300 dpi. This could guarantee a relatively accurate analysis but with a much faster analysis time. The root morphology together with root length density (RLD, defined as the length of roots per unit volume of soil) was then analysed using WinRhizo software (Regent Instruments, Canada). The total RLD for the whole root system was then back-calculated based on the dry weight (fraction of scanned samples compared to the total sample).

For the measurements of root distribution at the shear plane depths used in the shear test samples, the testing method and procedures reported by Loades et al. (2010) were employed. After shear testing, soil cores extruded from the shear box were carefully

Please cite this article in press as: Liang, T., et al., Scaling of the reinforcement of soil slopes by living plants in a geotechnical centrifuge. Ecol. Eng. (2017), http://dx.doi.org/10.1016/j.ecoleng.2017.06.067

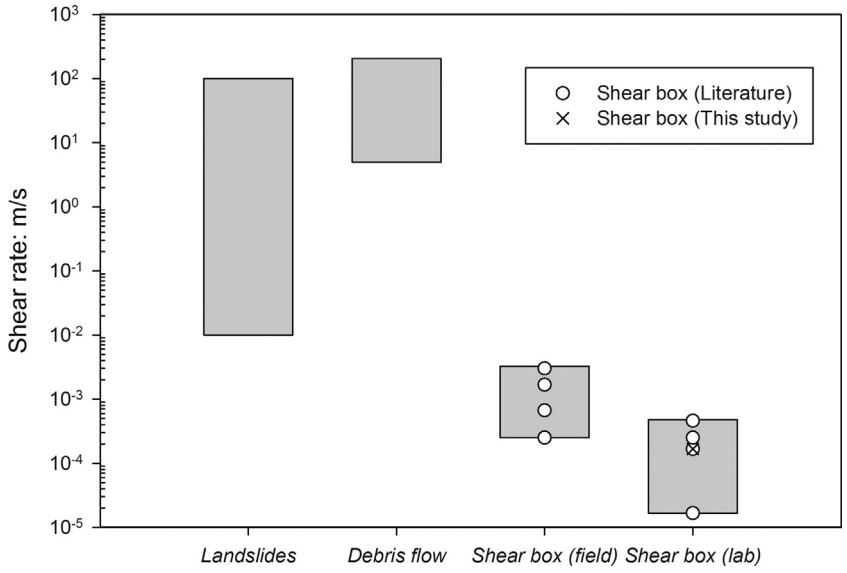

Fig. 3. Typical shear rates for landslides and debris flows (Davies et al., 2010), field shear box testing (Ekanayake et al., 1998; Cammeraat et al., 2005; Docker and Hubble, 2008; Fan and Su, 2008; Van Beek et al., 2005; Mickovski and Van Beek, 2009; Fan and Chen, 2010; many other studies do not provide adopted rates), laboratory shear box testing on root-reinforced soil (Waldron, 1977; Operstein and Frydman, 2000; Normaniza et al., 2008; Van Beek et al., 2005; Mickovski et al., 2009; Loades et al., 2010) and shear rates adopted in the present study, after Meijer et al. (2016).

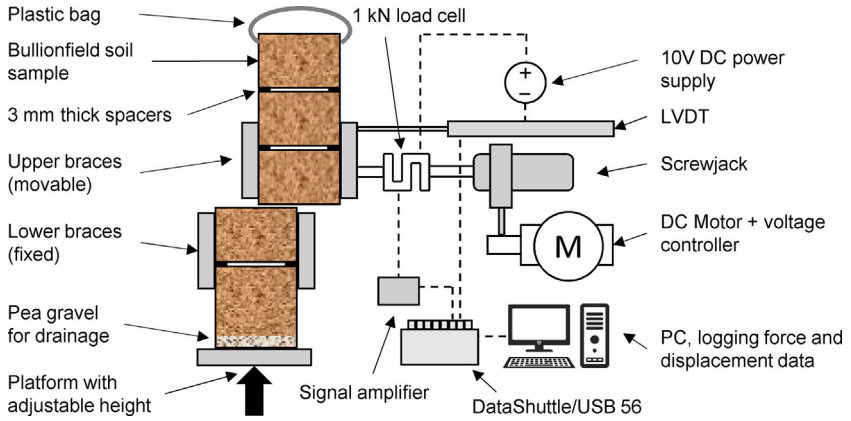

Fig. 4. Test setup for 150 mm diameter core laboratory direct shear apparatus at a shear plane of 300 mm.

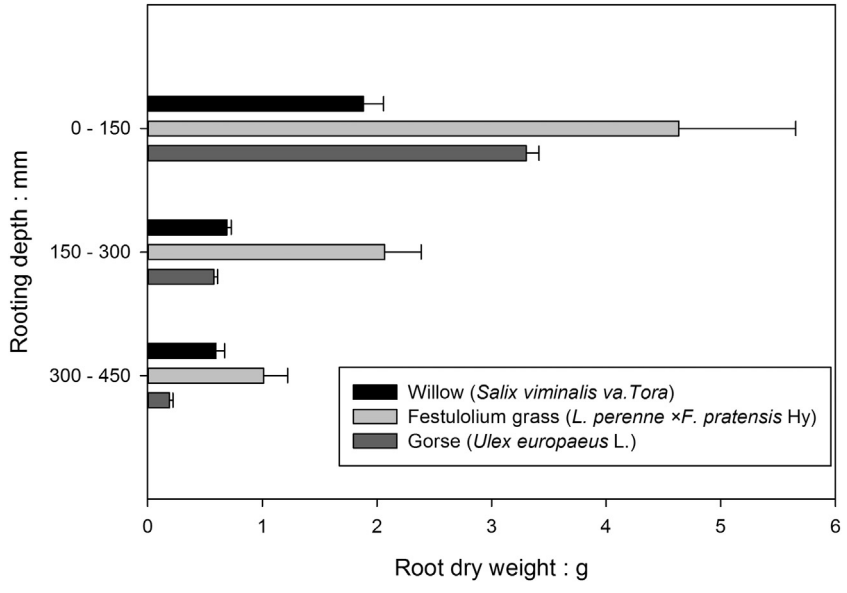

Fig. 5. Mean dry weights (±SE) of root biomass located at different soil depth for the three species.

Please cite this article in press as: Liang, T., et al., Scaling of the reinforcement of soil slopes by living plants in a geotechnical centrifuge. Ecol. Eng. (2017), http://dx.doi.org/10.1016/j.ecoleng.2017.06.067

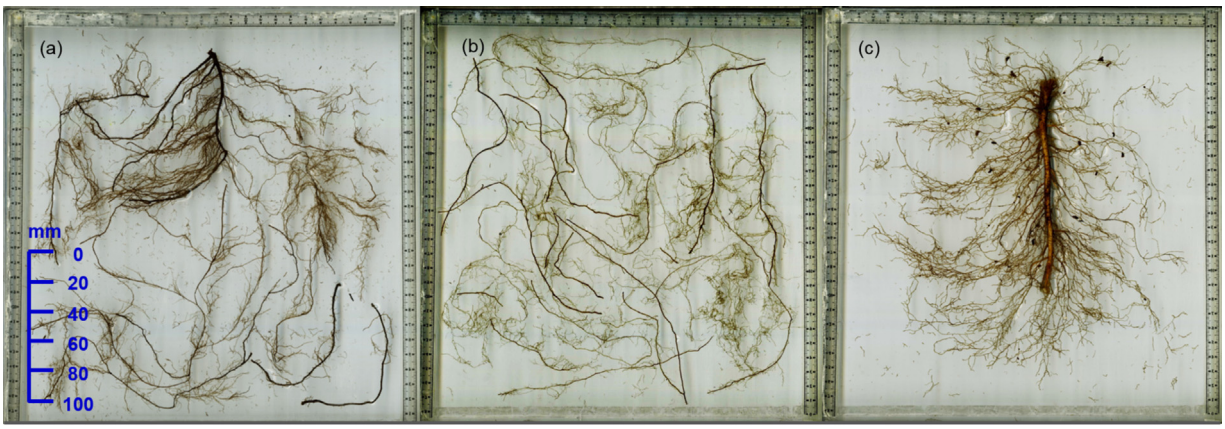

Fig. 6. The scanned root samples show root architecture: (a) Willow; (b) Festulolium grass; (c) Gorse.

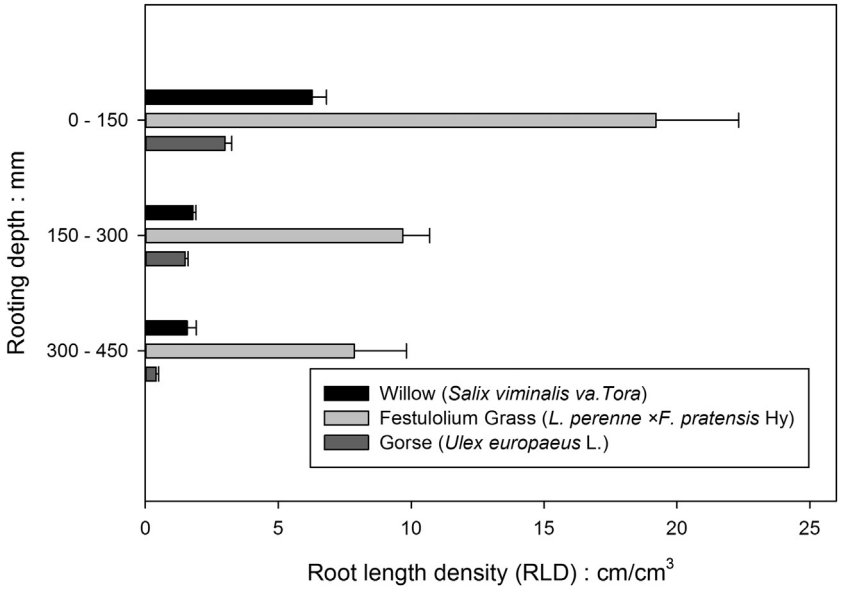

Fig. 7. Mean root length density (±SE) measured at different depth of the soil for the three species.

Table 2
Exponential fit parameters and R^2 values between peak root tensile strength/Young's modulus and diameter (Root tensile strength T_r/Young's modulus $E = A \times d^k$ where d = root diameter).

	Depth (mm)	Willow			Grass			Gorse		
		A	*k*	R^2	*A*	*k*	R^2	*A*	*k*	R^2
Tensile strength	In population	6.4835	0.032	0.0003	5.905	−0.596	0.1341	18.316	−0.03	0.0009
	0–150	6.0272	−0.074	0.0024	8.2185	−0.285	0.0317	23.991	0.0911	0.0001
	150–300	7.9222	−0.056	0.0007	5.0591	−0.921	0.3028	22.56	0.5764	0.0936
	300–450	8.503	1.1455	0.2163	2.5772	−1.358	0.6018	539.08	3.2149	0.2755
Young's Modulus	In population	97.181	0.0816	0.0027	62.625	−0.556	0.0982	533.37	0.2147	0.055
	0–150	79.09	−0.121	0.0072	84.023	−0.241	0.0176	582.8	0.0589	0.0012
	150–300	172.46	0.4187	0.0902	49.817	−1.019	0.2937	481.4	−0.4172	0.1192
	300–450	116.7	0.9886	0.2305	34.227	−1.074	0.3296	2732.2	−2.1644	0.2478

pushed back to their original position. The two shearing sections were then secured together using strong adhesive tape. Thereafter, each soil core was frozen at −20 °C. At the time of measurement, a diamond circular saw lubricated with water was used to cut the frozen cores into several sections. The cutting notch was slightly lower than the shear plane (by 2 mm), and warm water was applied to the exposed soil surface to remove the topmost soil and expose the roots across the shear plane. After placing a grid with 36 sectors (25 mm × 25 mm) over the shear plane, root numbers and root diameters were recorded visually using a microscope with an eyepiece graticule. Root area ratio (RAR), defined as the ratio between the cross-sectional area of roots crossing the shear plane and the total area of the shear plane, was calculated for all samples. It should be noted that the diameter used to calculate the total area of the shear plane was 145 mm instead of 150 mm. The reason for this is because roots that grew along the tube walls were severed with a surgical blade to 2.5 mm depth (see Section 2.7). This portion of roots was also not included when calculating RAR.

Please cite this article in press as: Liang, T., et al., Scaling of the reinforcement of soil slopes by living plants in a geotechnical centrifuge. Ecol. Eng. (2017), http://dx.doi.org/10.1016/j.ecoleng.2017.06.067

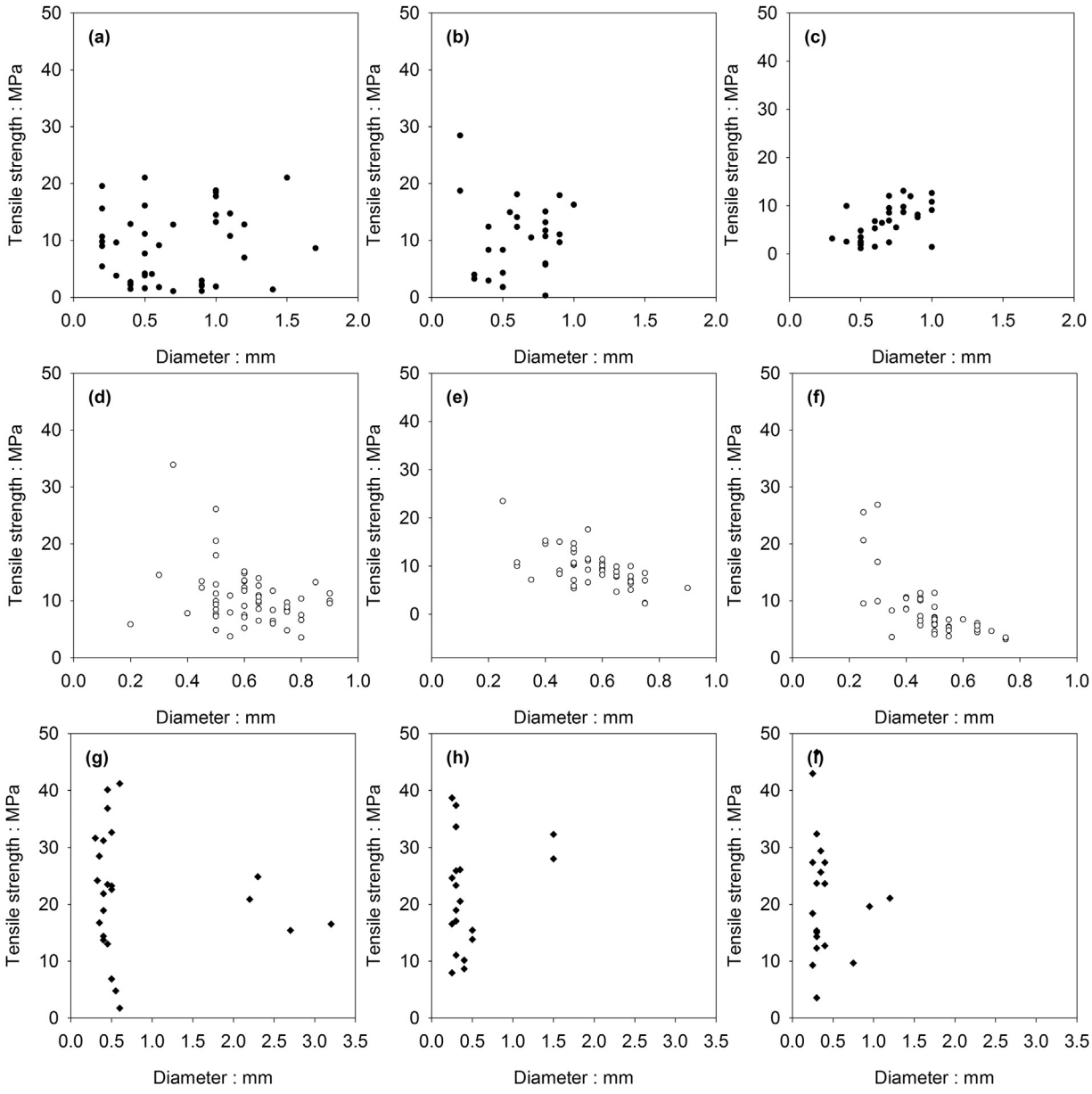

Fig. 8. Root tensile strength measured at different depth of the soil for the three species as a function of root diameter: (a)–(c) Willow; (d)–(f) Festulolium grass; (g)–(i) Gorse; the soil depth increases from left to right and represent 0–150 mm, 150–300 mm and 300–450 mm, respectively.

2.6. Tensile testing

A universal testing machine (INSTRON 5966, INSTRON, MA, USA) fitted with a 50-N load cell accurate to 2 mN was used to apply tensile loading to each root sample with an axial extension rate of 2 mm/min (Genet et al., 2005). Root samples that were no less than 100 mm length and with different diameters were used for testing. Both ends of the roots (20 mm length each) were secured with screw-thread grips. Tensile force and extension were recorded until each sample broke. The maximum force at failure and the cross-sectional area were used to calculate the root tensile strength (T_r). Root Young's modulus (E, root stiffness) was calculated from the initial slope of the stress-strain curve.

2.7. Direct shear testing

A shear table designed by Mickovski et al. (2009) was used to perform the direct shear tests in this study. The device allows for shearing of a 150 mm diameter circular container at any prescribed depth. Before each shear test, the soil core was fully saturated and left under free gravity drainage for 48 h until an equilibration of pore water pressure was achieved in the soil, ensuring a field capacity condition. During this process, the aerial parts of the plants were removed and each core was covered with a plastic bag or plastic wrap to minimize evapotranspiration effects on pore water pressure near the surface of the soil.

After the soil core was transferred onto the shear table, the adhesive tape that held the sections together and the spacers were carefully removed. A surgical scalpel blade was then used to cut the rim of the shear surface to a depth of 2.5 mm as mentioned above. For each soil core, the shear tests were performed from the bottom shear plane to the top shear plane to minimise the disturbance of roots in adjacent layers (e.g. pull out of deep roots). The fallow and planted samples were sheared at a constant shear rate of 1 mm/min in correspondence with root-reinforced soil shear box rates reported in the literature (Waldron, 1977; Ekanayake

Please cite this article in press as: Liang, T., et al., Scaling of the reinforcement of soil slopes by living plants in a geotechnical centrifuge. Ecol. Eng. (2017), http://dx.doi.org/10.1016/j.ecoleng.2017.06.067

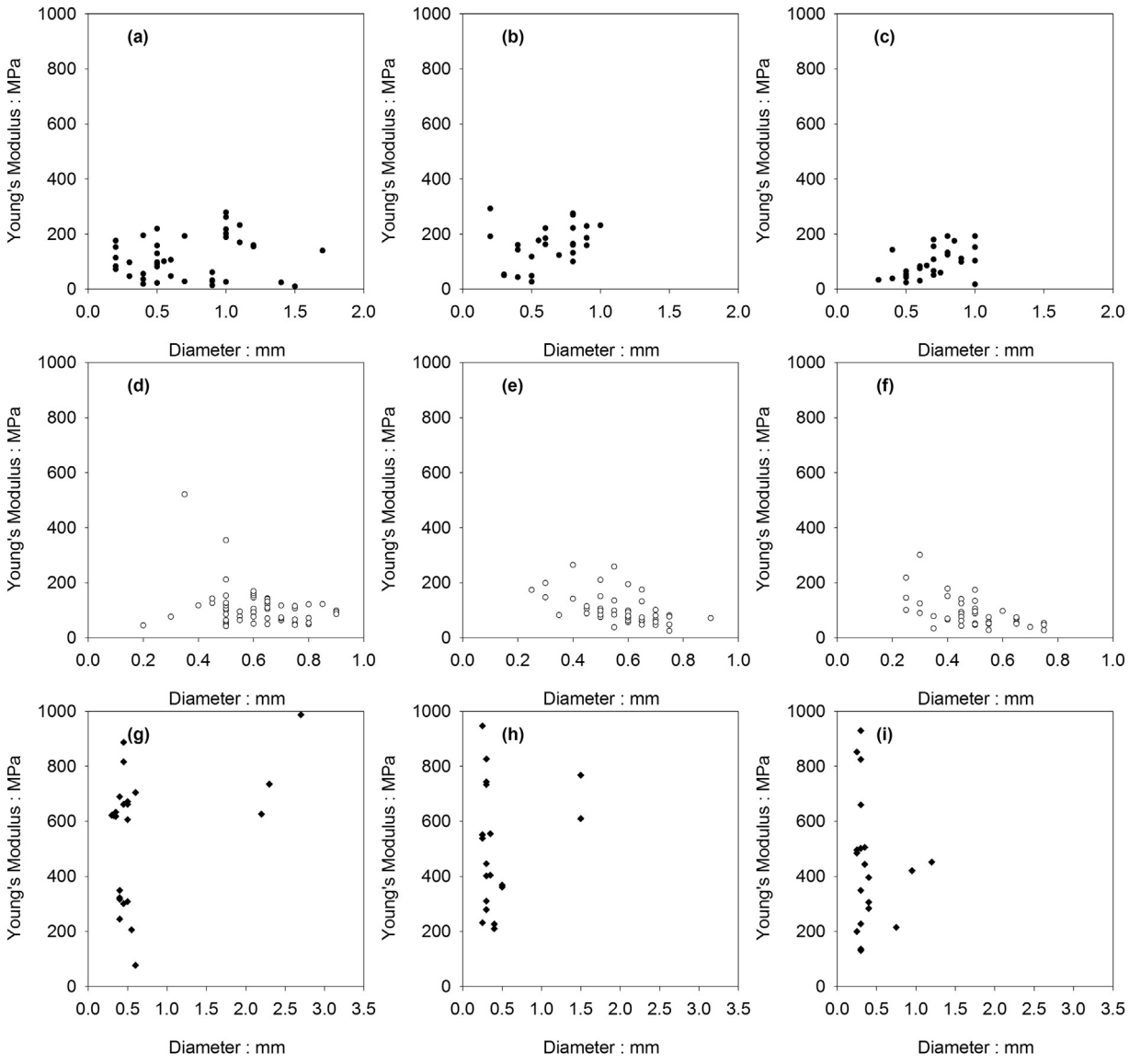

Fig. 9. Root Young's Modulus measured at different depth of the soil for the three species as a function of root diameter: (a)–(c) Willow; (d)–(f) Festulolium grass; (g)–(i) Gorse; the soil depth increases from left to right and represent 0–150 mm, 150–300 mm and 300–450 mm, respectively.

et al., 1998; Davies et al., 2010; Operstein and Frydman, 2000; Cammeraat et al., 2005; Docker and Hubble, 2008; Fan and Su, 2008; Normaniza et al., 2008; Van Beek et al., 2005; Mickovski et al., 2009; Mickovski and Van Beek, 2009; Fan and Chen, 2010; Loades et al., 2010) (see Fig. 3, after Meijer et al., 2016), until the maximum horizontal travel distance of the shear table (90 mm) was reached. Equipment limitations did not allow faster shear rates. The horizontal force was measured using a 1 kN ± 0.3 N load cell (RDP, UK) and the horizontal displacement was measured with a linear variable differential transformer (LVDT). Both the load cell and LVDT were calibrated prior to testing. Force and displacement data was logged during shearing using a USB data acquisition system DataShuttle/USB 56 (IOtech, Inc., USA). No additional normal stress was applied to the soil core, so the total normal stress at the shear plane was due to the self-weight of the soil above the shear plane. A typical shear test setup for a shear plane of 300 mm is shown in Fig. 4. After each shearing test, soil squeezed out during shearing was collected to measure the water content. Following that, the soil cores were pushed back to their original position, sealed and frozen for subsequent measurement of RAR, as mentioned in Section 2.3. The shear strength for the rooted samples was calculated as the measured shearing force divided by the total shear plane area (diameter 145 mm; rather than the effective shear plane). Peak shear strength was recorded both for rooted and fallow samples. The additional shear strength provided by roots was taken as the maximum difference in shear resistance between the rooted and fallow samples (i.e. subtracting the interpolated resistance curves at 0.1 mm displacement resolution, divided by the total shear plane area).

2.8. Data analysis

Statistical analyses were conducted using GenStat 15th edition (VSN International, Hemel Hempstead, UK). Significance testing for the root morphology and the bio-mechanical properties of the selected juvenile plants among replicates and samples were analysed using an analysis of variance (ANOVA) test. Relationships between root diameter and strength were fitted with power-law curves. Linear regression analyses were used to determine the relationship between RAR and the increased shear strength.

Please cite this article in press as: Liang, T., et al., Scaling of the reinforcement of soil slopes by living plants in a geotechnical centrifuge. Ecol. Eng. (2017), http://dx.doi.org/10.1016/j.ecoleng.2017.06.067

3. Results

3.1. Root morphology and properties

At the end of the growing period, the average dry weight of root biomass per core was 3.17 ± 0.19 g (Mean ± SE), 7.71 ± 1.43 g, 3.31 ± 0.11 g for Willow, Festulolium grass and Gorse, respectively. For all three species, the root dry biomass decreased significantly with an increase in soil depth (Fig. 5) ($P < 0.05$). Root biomass in the top soil (<150 mm) occupied 60%. 70% and 80% of the total amount (roots above 450 mm) for Willow, Festulolium grass and Gorse, respectively. The three species developed significantly different root morphology (see Fig. 6). Festulolium grass has a typical fibrous root system (Fig. 6b); Gorse has a tap root system that consists of a main thicker tap root where numerous secondary roots less than 0.5 mm in diameter were attached (Fig. 6c); and Willow developed a root system with numerous branches of different diameters (Fig. 6a). Significant differences in the mean RLD were observed among the three species ($P < 0.001$). The RLD per core was 9.6 ± 0.85 cm/cm^3, 36.7 ± 4.7 cm/cm^3, 4.9 ± 0.19 cm/cm^3 for Willow, Grass and Gorse, respectively. RLD was found to decrease with rooting depth for all three species (Fig. 7; $P < 0.001$, $P < 0.05$, $P < 0.001$, for Willow, Festulolium grass and Gorse, respectively).

3.2. Root biomechanical properties

The measured root tensile strength and Young's modulus as a function of root diameter are shown in Figs. 8 and 9, respectively. No clear correlations between the tensile strength or Young's modulus and root diameter for juvenile roots can be found directly from the figures. Conventionally-used power-law relationships were used to fit the data. The fitted R^2 values, between tensile strength and diameter are shown in Table 2. No matter how the data are fitted (either by population or depth), the R^2 values were very low for Willow and Gorse. R^2 values were poor (0.1341) when fitted to all roots in the population for Festulolium grass, however, when fits were restricted to rooting depth this improved for roots below 150 mm depth. Similar trends were found for Young's Modulus. Young's modulus increased strongly with root tensile strength (R^2 of 0.55, 0.69, 0.50 for Willow, Festulolium grass and Gorse, respectively), as shown in Fig. 10.

Roots were grouped into four diameter classes (0–0.5 mm, 0.5–0.75 mm, 0.75–1 mm and >1 mm), and the measured mean root tensile strength at each diameter class for the three species are shown in Fig. 11. No significant difference in the tensile strength of roots were observed between roots within different diameter ranges for Willow and Gorse ($P > 0.05$, $F = 1.10$, $df = 95$; $P > 0.05$, $F = 0.55$, $df = 63$; for Willow and Gorse, respectively), while for Festulolium grass, significant differences were observed ($P < 0.01$, $F = 6.58$, $df = 146$). The average root tensile strength for all the samples was 8.70 ± 0.60 MPa (Mean ± SE), 9.50 ± 0.40 MPa, 21.67 ± 1.29 MPa for Willow, Festulolium grass and Gorse, respectively. In contrast, Young's modulus differed significantly with root diameter for all three species ($P < 0.05$, $F = 3.85$, $df = 95$; $P < 0.01$, $F = 5.51$, $df = 146$; $P < 0.01$, $F = 4.46$, $df = 63$; for Willow, Festulolium grass and Gorse, respectively).

Within each root diameter class, root tensile strength and Young's modulus were correlated with soil depth. Table 3 summarises the difference of the statistics of the regression. No significant difference was observed both in root tensile strength and Young's modulus for 0–0.5 mm diameter roots sampled at different depths (0–150 mm, 150–300 mm and 300–450 mm). This was the case for all three species with an exception for Young's modulus of Gorse. On the contrary, for 0.5–0.75 mm diameter roots, soil depth was found to significantly affect root tensile strength and

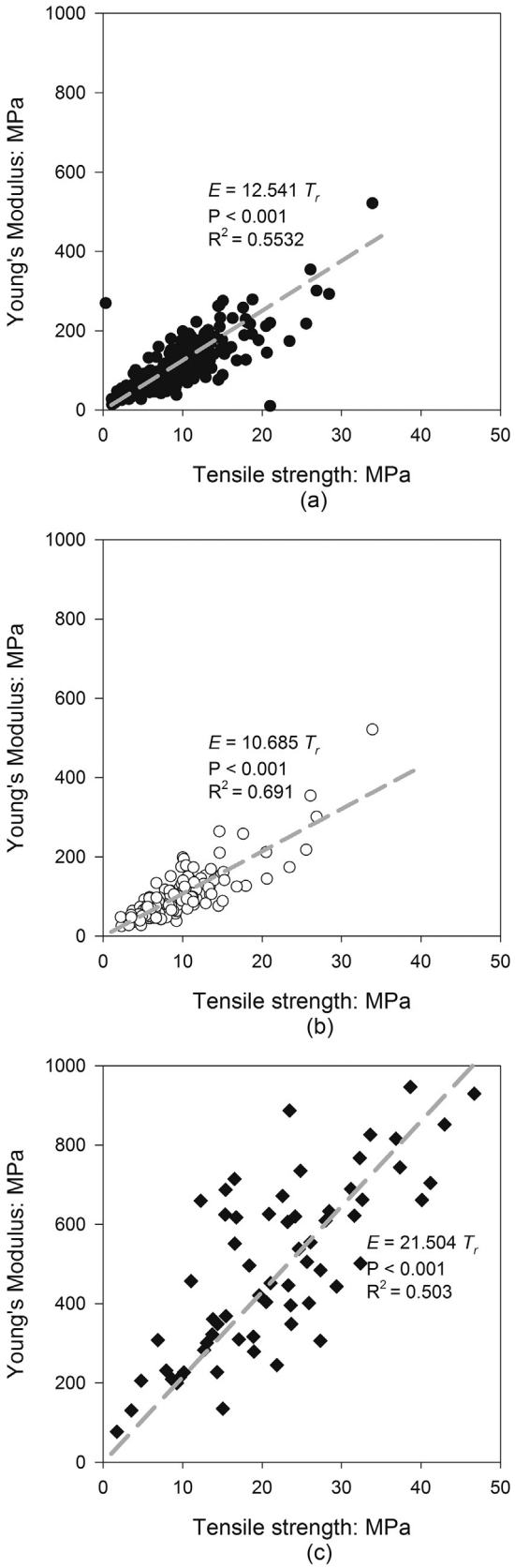

Fig. 10. Correlation between root Young's modulus and root tensile strength: (a) Willow; (b) Festulolium grass; (c) Gorse.

Please cite this article in press as: Liang, T., et al., Scaling of the reinforcement of soil slopes by living plants in a geotechnical centrifuge. Ecol. Eng. (2017), http://dx.doi.org/10.1016/j.ecoleng.2017.06.067

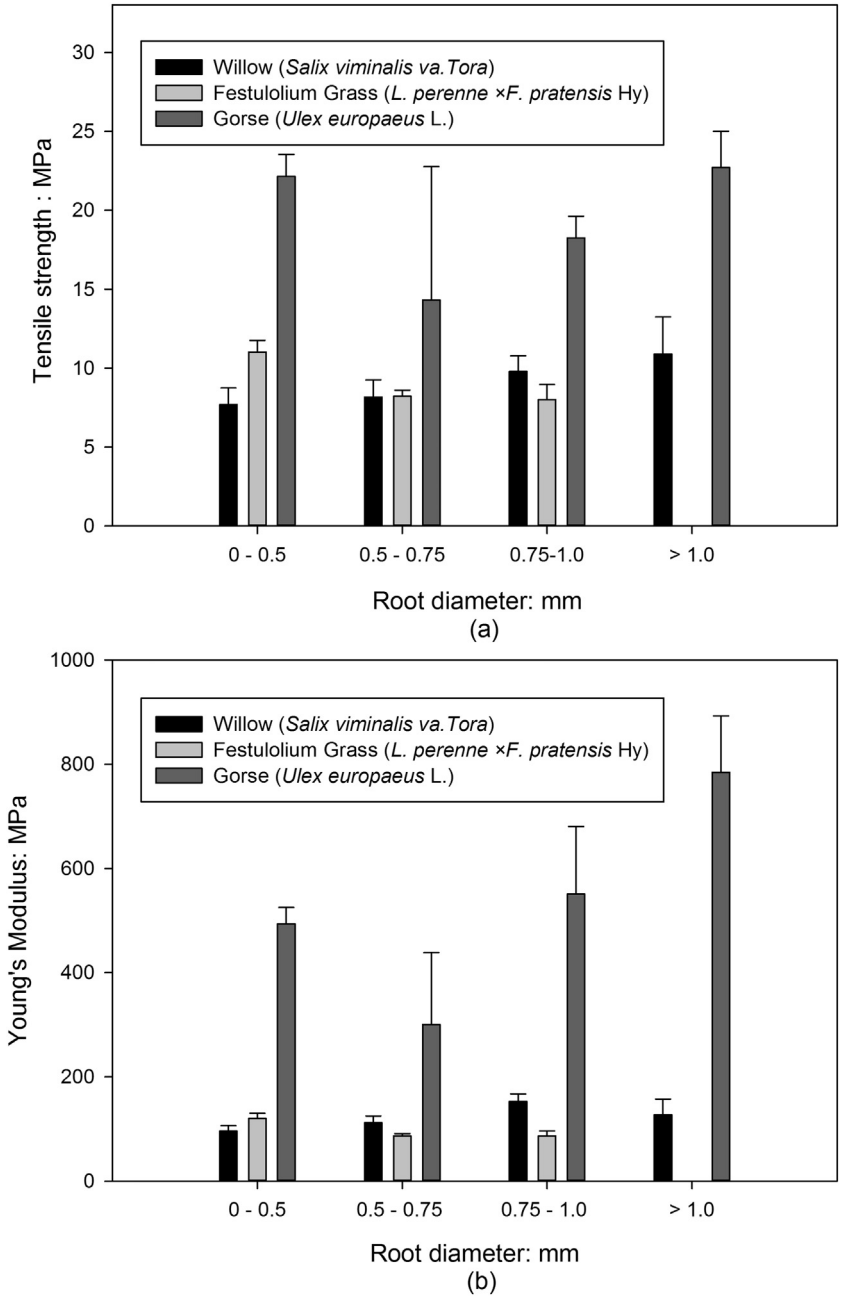

Fig. 11. Mean root biomechanical properties (±SE) for root samples within different diameter range: (a) Tensile strength; (b) Young's Modulus.

Table 3
P values for significant differences in root tensile strength and Young's modulus as a function of soil depth at each root diameter class (Results of ANOVA).

	Diameter (mm)	Willow	Grass	Gorse
Tensile strength	0–0.5	*n.s*	*n.s*	*n.s*
	0.5–0.75	<0.01**	<0.001***	/
	0.75–1	*n.s*	/	/
Young's Modulus	0–0.5	n.s	n.s	<0.01**
	0.5–0.75	<0.05*	<0.01**	/
	0.75–1	*n.s*	/	/

n.s not significant.
* $P < 0.05$.
** $P < 0.01$.
*** $P < 0.001$.

Please cite this article in press as: Liang, T., et al., Scaling of the reinforcement of soil slopes by living plants in a geotechnical centrifuge. Ecol. Eng. (2017), http://dx.doi.org/10.1016/j.ecoleng.2017.06.067

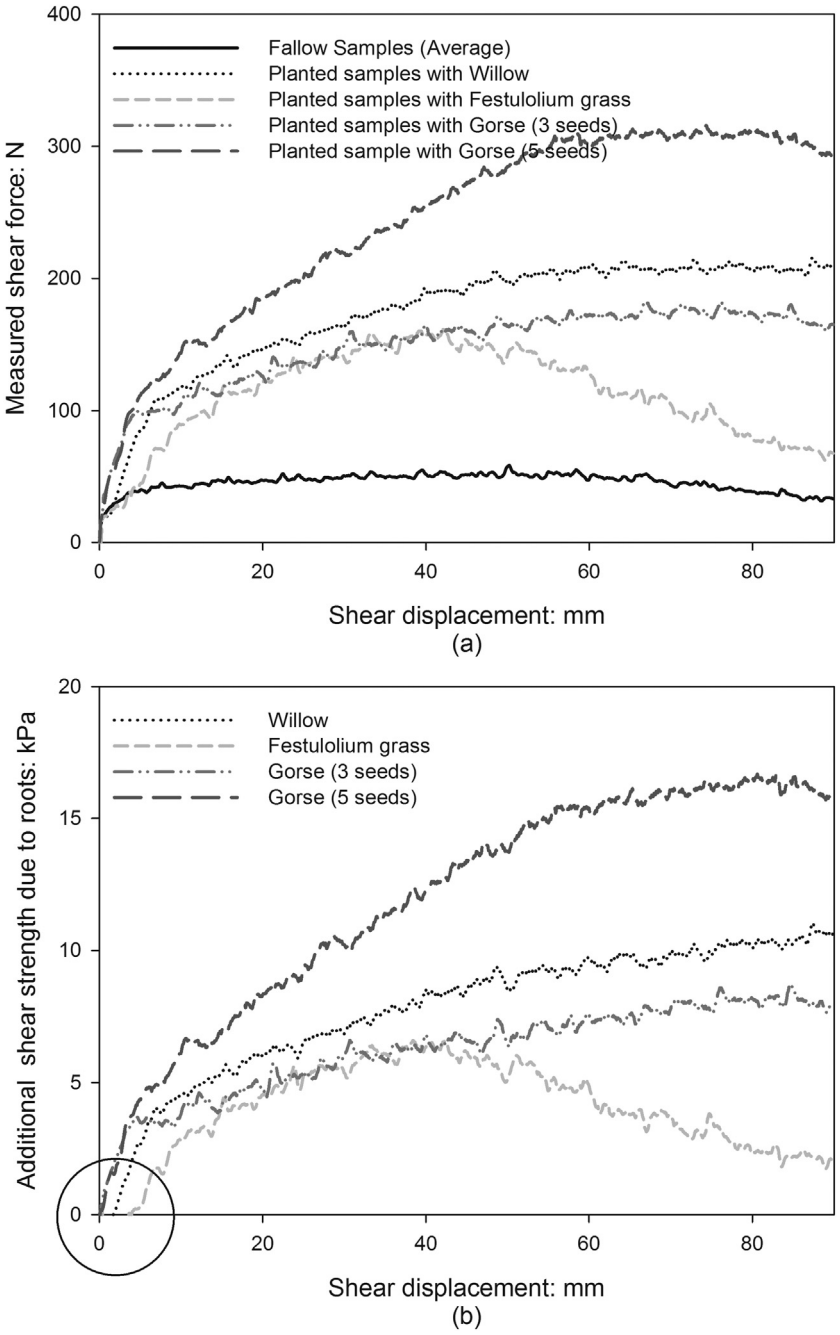

Fig. 12. (a) Typical experimental results of shear resistance versus shear displacement relationship for soil samples permeated with roots of different plant species; (b) Additional shear strength provided by roots, which was estimated as the interpolated shear resistance (over a uniformly-spaced values of displacement of 0.1 mm) difference between the rooted sample and fallow sample (average value) over the total shear plane area.

Young's modulus, both for Willow and Festulolium grass. Correlations for Gorse were not assessed because its roots consisted of a main tap root and root diameter less than 0.5 mm.

3.3. Direct shear tests

The average soil water content and degree of saturation at each shear plane was similar for fallow and planted samples and did not vary significantly between species ($P > 0.05$, Table 4). A typical shear resistance–shear displacement relationship across the shear plane at 100 mm for each of the plant species tested in this study is shown in Fig. 12. The additional shear strength provided by roots was also plotted here as the difference in shear resistance over the total shear plane area between the rooted and fallow samples. A certain shear strain was required before the additional shear strength started to be active (see Fig. 12b), which varies with the species (1.7 mm, 3.6 mm and 0 mm for Willow, Festulolium grass and Gorse, respectively). The maximum additional shear resistance was mobilized at a large shear deformation for all three species (56 mm, 40 mm and 55 mm for Willow, Festulolium grass and Gorse, respectively). It is interesting to note that the shape of the shear resistance-displacement curves differed between species: A clear post-peak reduction was observed for Festulolium grass, while for Willow and Gorse, the additional shear resistance remained constant with continuous shearing once the maximum shear additional shear resistance was mobilized.

Please cite this article in press as: Liang, T., et al., Scaling of the reinforcement of soil slopes by living plants in a geotechnical centrifuge. Ecol. Eng. (2017), http://dx.doi.org/10.1016/j.ecoleng.2017.06.067

Table 4
The measured soil water content (g/100 g) and degree of saturation (m^3/m^3) at each shear plane after shear tests (Mean ± SE).

Shear depth (mm)	Fallow	Willow	Grass	Gorse
100	19.75 ± 0.21 (0.59 ± 0.01)	22.29 ± 1.06 (0.66 ± 0.03)	20.76 ± 0.77 (0.62 ± 0.02)	19.1 ± 0.31 (0.57 ± 0.01)
200	23.81 ± 0.14 (0.71 ± 0.00)	23.59 ± 0.73 (0.70 ± 0.02)	24.02 ± 0.59 (0.71 ± 0.02)	22.22 ± 0.08 (0.66 ± 0.02)
300	25.95 ± 0.10 (0.77 ± 0.00)	25.13 ± 0.69 (0.75 ± 0.02)	26.34 ± 0.21 (0.78 ± 0.01)	25.64 ± 0.29 (0.76 ± 0.01)
400	27.11 ± 0.17 (0.80 ± 0.00)	26.46 ± 0.62 (0.79 ± 0.02)	27.45 ± 0.48 (0.81 ± 0.01)	27.35 ± 0.03 (0.81 ± 0.00)

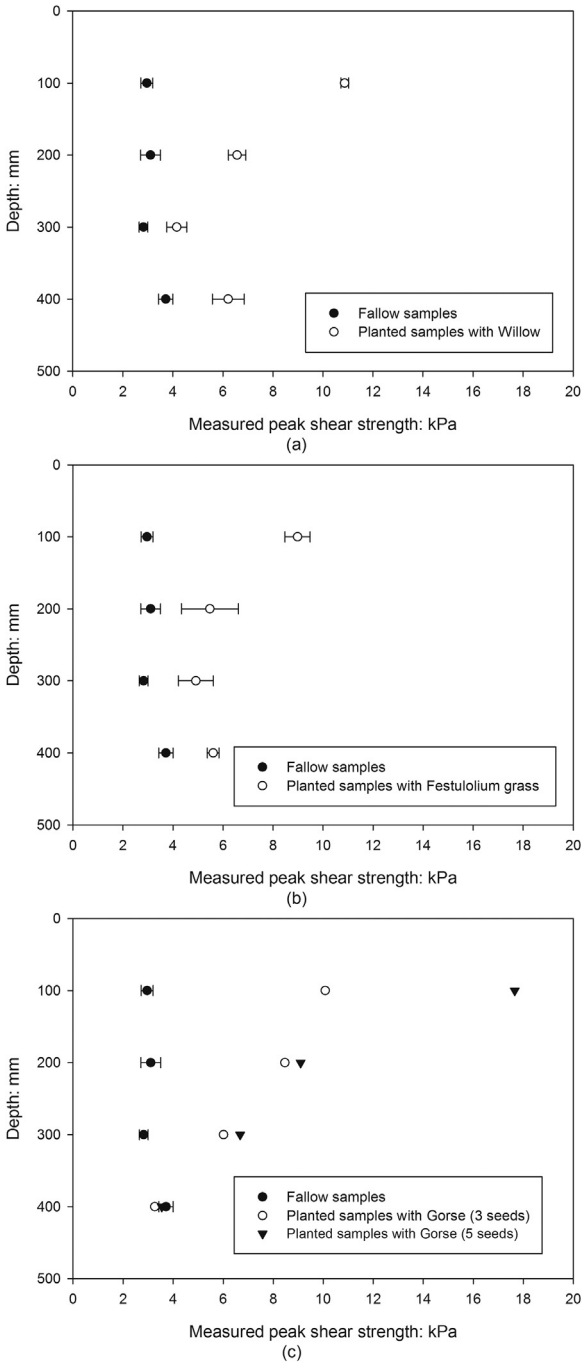

Fig. 13. The measured shear strength (±SE) for fallow and rooted samples: (a) Willow; (b) Festulolium grass; (c) Gorse.

Fig. 13 shows a comparison of the measured peak shear strength between rooted and fallow samples. It should be noted that for the three replicates planted with Gorse, only one of them successfully developed all five healthy young plants, while one developed three heathy seedlings and no plants survived in the last core. Therefore, only test results for five and three Gorse plants/core are presented in Fig. 12c. In all cases, the peak shear strength of fallow samples always increased with depth and was less than the strength of the rooted samples. In contrast, the peak strength of rooted samples decreased with increasing shear depth below 300 mm, for all three species. At 400 mm depth, the results differed between species. The strength of soil vegetated with Willows and Festulolium grass began to follow the trend of the fallow tests, while the Gorse continued to decrease with depth.

The root properties at the shear plane for rooted samples are shown in Table 5. For deeper shear depths, no significant differences were observed for root number ($P > 0.5$), but the total root cross sectional area, and thus, RAR, decreased significantly with increasing shear depth below 300 mm depth ($P < 0.001$; Fig. 14). Roots thinner than 0.25 mm diameter represented more than 75% of the total root number, but less than 20% of RAR. In contrast, fewer than 2% of roots counted were >1 mm diameter, yet these accounted for up to 60% of RAR. Larger mean RAR values were observed at the 400 mm depth than at 300 mm depth for both for Willow and grass, which presumably explain in the larger root shear strength. The shear strength increase for each sample at each shear plane (c_r) is plotted against RAR in Fig. 15. For all three species a clear positive linear relationship between c_r and RAR can be described by:

$$c_r = k \cdot A_r \cdot T_r \quad (2)$$

where A_r is root area ratio; T_r is the average tensile strength; k is root soil interaction factor taking account of root orientation and root breaking process (Meijer, 2016), $k = 1.15$ is assumed in WWM (Wu, 1976; Waldron, 1977), however, WWM generally overestimates the root reinforcement; k values ranging from 0.25 to 1.15 have been reported by an extensive of laboratory or in situ studies (e.g. Operstein and Frydman, 2000; Pollen and Simon, 2005; Bischetti et al., 2009; Hales et al., 2009; Schwarz et al., 2010c; Comino et al., 2010; Mao et al., 2012; Adhikari et al., 2013).

Based on the mean tensile strength reported above (8.70 MPa, 9.50 MPa, 21.67 MPa for Willow, Festulolium grass and Gorse, respectively), k value of 0.312, 1.07 and 0.318 was found for Willow, Festulolium grass and Gorse, respectively:

$$\text{Willow}: c_r = 0.312 \cdot A_r \cdot T_r, R^2 = 0.8321 \quad (3)$$

$$\text{Festuloliumgrass}: c_r = 1.07 \cdot A_r \cdot T_r, R^2 = 0.8763 \quad (4)$$

$$\text{Gorse}: c_r = 0.318 \cdot A_r \cdot T_r, R^2 = 0.9293 \quad (5)$$

Roots thinner than 0.5 mm diameter represented more than 90% of the total root number for all three species (see Fig. 14), if the correlation between c_r and RAR was fitted with the mean tensile strength of roots thinner than 0.5 mm (7.69 MPa, 11.03 MPa, 21.85 MPa for Willow, Festulolium grass and Gorse, respectively, see Fig. 11a), k value of 0.354, 0.925 and 0.33 was found for Willow, Festulolium grass and Gorse, respectively.

4. Discussion

4.1. Modelling root morphology and rooting depth

Distinct and contrasting root morphology was observed for the three species (Fig. 6), which is important for modelling

Table 5
Root system properties recorded on the shear surface of the planted sample, CSA refers to cross sectional area and RAR to root area ratio (Mean ± SE).

Species	Shear depth (mm)	Total number of roots	Total CSA, mm^2	RAR (%)	Mean root diameter, mm
Willow	100	177 ± 18.82	49.79 ± 4.37	0.302 ± 0.027	0.389 ± 0.046
	200	258 ± 2.65	18.40 ± 2.75	0.111 ± 0.017	0.216 ± 0.015
	300	125 ± 9.84	4.93 ± 1.24	0.030 ± 0.008	0.172 ± 0.007
	400	145 ± 13.20	7.41 ± 0.89	0.045 ± 0.005	0.198 ± 0.005
Grass	100	394 ± 28.69	9.72 ± 0.72	0.059 ± 0.004	0.141 ± 0.001
	200	369 ± 20.31	6.54 ± 0.93	0.040 ± 0.006	0.128 ± 0.004
	300	316 ± 26.52	4.04 ± 0.46	0.024 ± 0.003	0.114 ± 0.002
	400	316 ± 12.99	3.95 ± 0.59	0.024 ± 0.004	0.113 ± 0.004
Gorse (3 seeds)	100	147	20.99	0.127	0.279
	200	117	10.27	0.062	0.254
	300	105	5.23	0.032	0.225
	400	93	2.84	0.017	0.192
Gorse (5 seeds)	100	156	34.77	0.211	0.326
	200	147	19.09	0.116	0.279
	300	139	8.84	0.054	0.245
	400	45	3.16	0.019	0.271

slope behaviour in the centrifuge considering the significant root morphology effects on soil reinforcement (Fan and Chen, 2010; Ghestem et al., 2014b). Evaluation of the similarities and differences between the root morphology of juvenile and mature plants is required to improve the use of juvenile plants in centrifuge modelling (Docker and Hubble, 2009).

Previous investigation into the contribution of roots on soil shear strength conventionally focused on the top 1–2 m soil layers, because most of the root biomass was found within the surface 50 cm. According to a global analysis of root distributions for terrestrial biomes, approximately 30%, 50% and 75% of root biomass is found in the top 10 cm, top 20 cm and top 40 cm, respectively (Jackson et al., 1996). Technological limitations also restrict access to deeper soil layers for shear testing in the field. Although only a small fraction of root biomass might be found at depths below 1m, the root contribution to soil shear strength at those depth could still be significant. For example, at a test depth of 1 m, the derived soil shear strength increase based on measured RAR for European larch, European beech, European hop-hornbeam, sweet chestnut and Norway spruce were 12.7 kPa, 9.3 kPa, 6.3 kPa, 5.7 kPa and 2.6 kPa, respectively, according to a field survey in the Italian Alps by Bischetti et al. (2009). To more accurately model mechanical root contributions on slope stability, the deep rooting habit of plants and its function against deep seated instability should be considered (Docker and Hubble, 2008). Canadell et al. (1996) compiled 290 observations of maximum rooting depth which covered 253 woody and herbaceous species and found that the maximum rooting depth for trees, shrubs and herbaceous plants was 7.0 ± 1.2 m, 5.1 ± 0.8 m and 2.6 ± 0.1 m, respectively (although this may often be restricted by shallow soil depths). The juvenile plants tested in this study reached the rooting depth of 450 mm for all three species at model scale. However, the lateral constraints of the 150 mm tubes used in this study prevented the lateral spread of the root systems and may contribute to a bias towards deep rooting; especially for Willow and Festulolium grass, considering their root morphology (see Fig. 6). This was checked by growing Willow and Festulolium grass within a 45° slope model in a centrifuge strong box liner under the same growing conditions as the tubes. Both Willow and Festulolium grass reached the same maximum model rooting depth as in the tubes, as shown in Fig. 16. If those plants (450 mm rooting depth) are being tested in a 1:N scale model in a centrifuge at a gravitational acceleration of N g, to match the maximum depths observed in the field, the corresponding largest scale factor N that could reasonably be modelled is 16, 12 and 6 for Willow, Gorse and Festulolium grass, respectively.

In terms of the distribution of root biomass, approximately 60%, 70% and 80% of roots were found in the uppermost soil layer (<2.25 m at prototype scale for an indicative N of 15), for Willow, Gorse and Festulolium grass, respectively. These values are relatively smaller compared with those of field species at the homologous depths (Jackson et al., 1996). However, all three species showed a consistent decreasing trend of root biomass with increasing depth which is typically found for mature plants (see Fig. 5).

4.2. Modelling root biomechanical properties

The measured mean values of root tensile strength and Young modulus for roots within different diameter ranges were scaled up according to scaling laws in Table 1 using an indicative scale of 15 and plotted against the upper and lower bounds of mature root data collated from the literature (Fig. 17). Here the mature field root tensile strength data (n = 40, 12 and 21 for trees, shrubs and grasses/herbs, respectively) were mainly collated from the database reported by Mao et al. (2012). However this database did not collect R^2 values of power-law relationship between strength and diameter, so the source documents were used to remove data with R^2 values less than 0.15 (after Loades et al., 2013). Data for Young's modulus of mature field roots is rare (n = 6, 5 and 2 for trees, shrubs and grasses/herbs respectively) and were collected from the following literature: Operstein and Frydman (2000), Van Beek et al. (2005), Mickovski et al. (2009), Fan and Su (2008), Teerawattanasuk et al. (2014). To avoid any mismatches of the actual root strength and stiffness in the field, the root tensile strength and Young's modulus of juvenile root prototypes should fall within the collected range of mature plants, and the maximum permitted scale N for Willow and Festulolium grass to achieve this are calculated to be more than 60, which is a typical scale for slope stability problems using centrifuge methodology (Take and Bolton, 2011). In contrast, a relatively small scale is permitted for Gorse, N = 12 and N = 2 for tensile strength and Young's modulus, respectively. The extremely low N value for Young's modulus of gorse may result from the insufficient field data on root Young's modulus compared with those on tensile strength. It may also suggest that younger roots (i.e. a growth period shorter than 3 months) may be desirable for gorse if it is used for centrifuge modelling.

Root tensile strength has been commonly assumed to be diameter dependant, typically following negative power-law curves across mixed populations of roots sampled (Bischetti et al., 2005). However, in this study the R^2 values of power-law relationships between strength and diameter were relatively low for all three

Please cite this article in press as: Liang, T., et al., Scaling of the reinforcement of soil slopes by living plants in a geotechnical centrifuge. Ecol. Eng. (2017), http://dx.doi.org/10.1016/j.ecoleng.2017.06.067

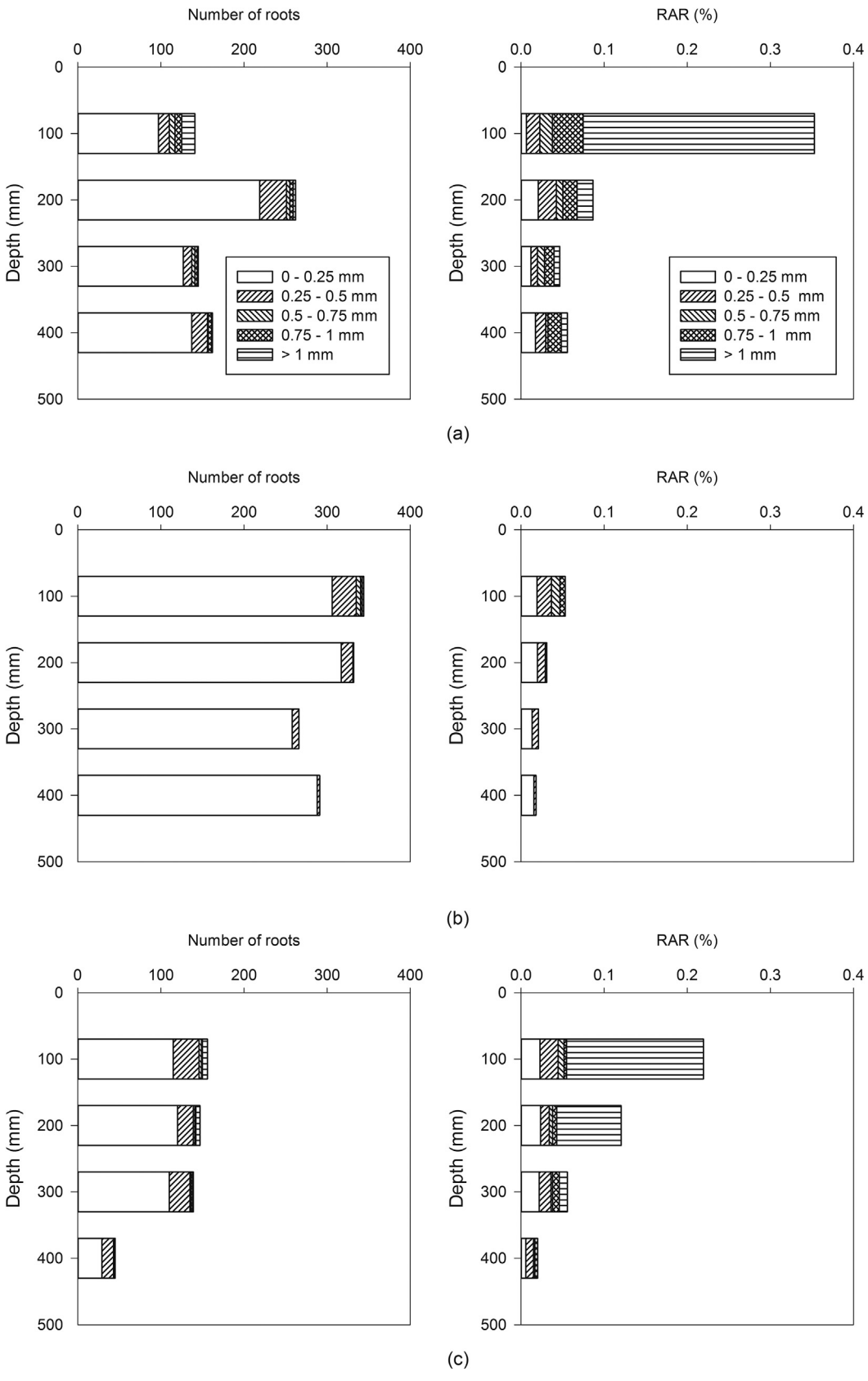

Fig. 14. The distribution of root biomass crossing the shear plane: root number and root cross sectional area (CSA): (a) Willow; (b) Festulolium grass; (c) Gorse.

species, which may be a combined result of root type and age, as all the tensile tests were performed on combined populations of roots (Loades et al., 2013, 2015). If the root samples are further classified by root age and root type, the R^2 values using negative power laws might be improved (Loades et al., 2013). However, it is also possible that the power-law relationship is often not suitable for

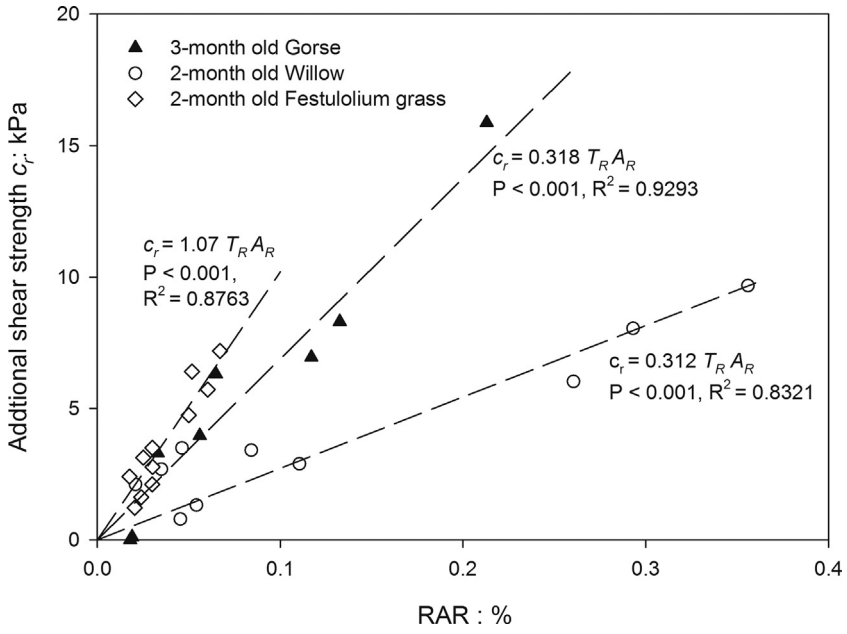

Fig. 15. Correlation between additional shear strength and the root area ratio crossing the shear plane.

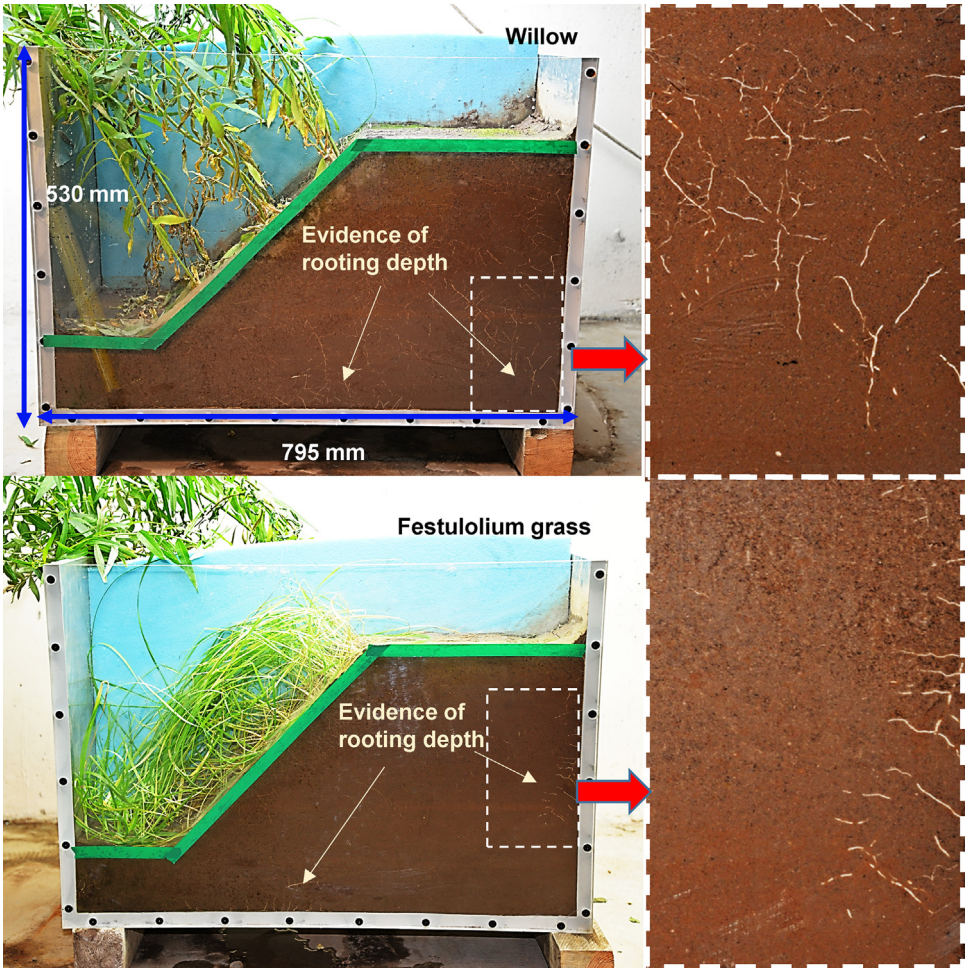

Fig. 16. The 2-month root growth conditions of Willow and Festulolium grass planted within the 1:1 slope model in centrifuge strong box under the same growing conditions with the 150 mm diameter tube tests. During the plant growing period, the centrifuge strong box was tilted by 45° to make the slope surface parallel to the ground to more realistically simulate the filed hydrological conditions.

Please cite this article in press as: Liang, T., et al., Scaling of the reinforcement of soil slopes by living plants in a geotechnical centrifuge. Ecol. Eng. (2017), http://dx.doi.org/10.1016/j.ecoleng.2017.06.067

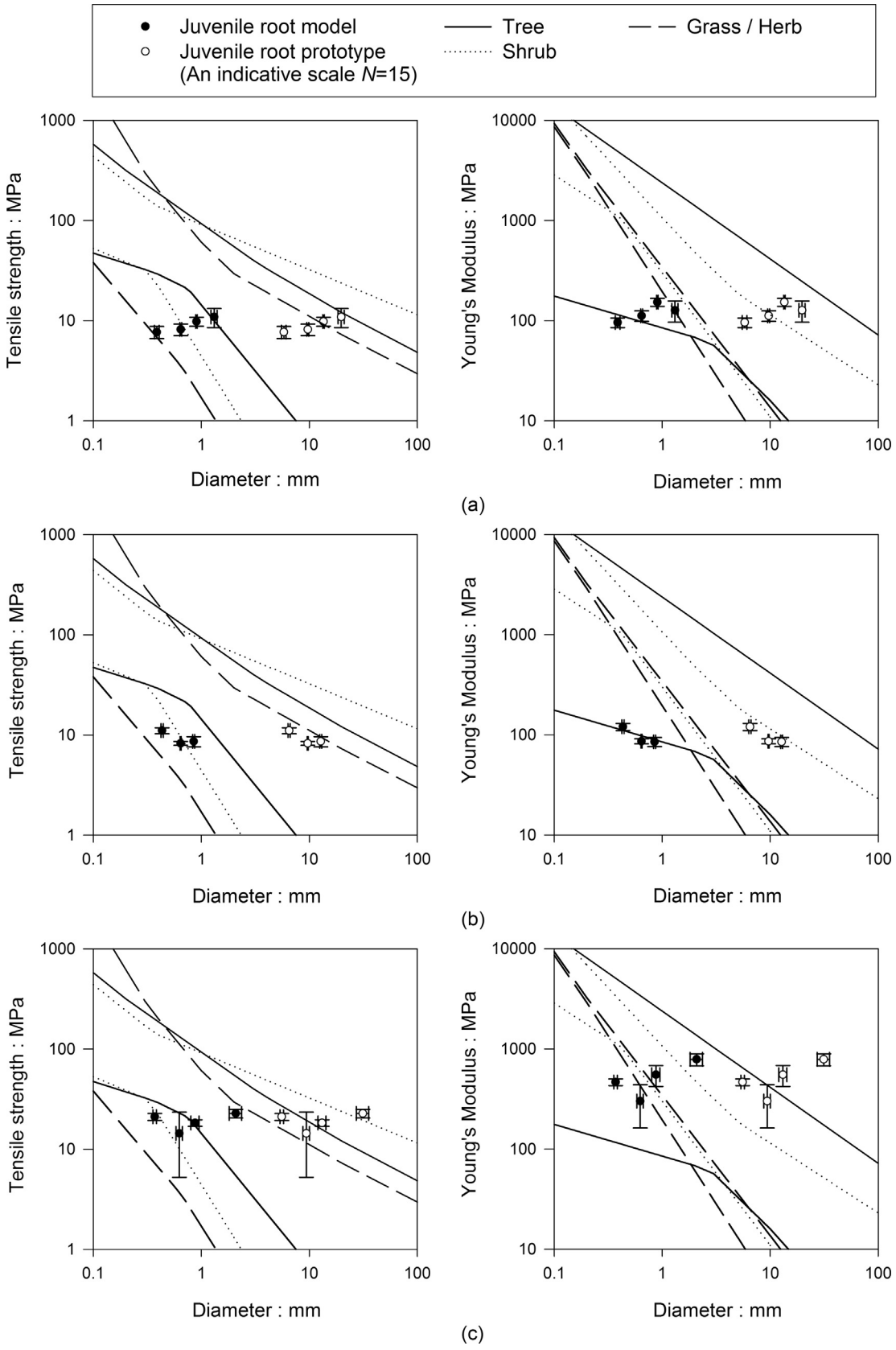

Fig. 17. Comparison of root biomechanical properties between the juvenile plants cultivated in this study and mature plants collected from the literature (Root tensile strength data, n = 40, 12 and 21 for trees, shrubs and grasses/herbs, respectively; Root Young's Modulus data, n = 6, 5 and 2 for trees, shrubs and grasses/herbs, respectively): (a) Willow; (b) Festulolium grass; (c) Gorse.

Please cite this article in press as: Liang, T., et al., Scaling of the reinforcement of soil slopes by living plants in a geotechnical centrifuge. Ecol. Eng. (2017), http://dx.doi.org/10.1016/j.ecoleng.2017.06.067

characterising root samples from juvenile plants. Actually, there is a lack of information and understanding of root biomechanical properties during the early stages of plant establishment. Even for mature plants, a large fraction of the variability in tensile strength-diameter relationship cannot be explained by negative power-law relationships and the physical basis of such relationships is still not clear (Mattia et al., 2005; Ghestem et al., 2014a; Boldrin et al., 2017b).

A strong linear relationship was found between root tensile strength and root Young's modulus of juvenile plants for all three tested species. Further work is required to identify the reasons for these relations and whether the root samples from mature plants of the same species exhibit similar characteristics.

4.3. Modelling root reinforcement

The soil water content at a given shear plane was similar between fallow and planted samples, so any difference in the shear strength of fallow and rooted soil was attributable to the mechanical root reinforcement. However, the soil water content varied between shear planes within a sample (see Table 4), specifically, the soil degree of saturation decreased from the bottom layer to the top layer. Such conditions might differ from those after heavy rainfall on a slope when the upper layers of soil are fully saturated. Previous studies on the influence of water content on root biomechanical contribution (e.g. Simon and Collison, 2002; Pollen, 2007; Fan and Su, 2008) found that when the soil water content (saturation) increased, the fallow soil sample became weaker, but the shear strength of the planted sample did not change – because the root contribution increased as the soil became wetter (Veylon et al., 2015). Hence the increased shear strength measured at each unsaturated root-reinforced shear plane could underestimate the contribution of root reinforcement under fully saturated conditions after rainfall.

Willow started to mobilize its additional shear strength at a shear strain, higher than Gorse, but lower than Festulolium grass (see Fig. 12b), which is exactly in the reverse order of root stiffness (see Fig. 11b). The role of root stiffness and root–soil adhesion on the mobilization of root reinforcement has been highlighted by Mickovski et al. (2007) and Schwarz et al. (2010a). The significant difference in shear resistance-shear displacement curves between species shown in Fig. 12 is not surprising and similar results have been reported by certain authors (e.g. Docker and Hubble, 2008; Fan and Chen, 2010; Ghestem et al., 2014b), which can be related to the root morphology and architecture of these species. According to Docker and Hubble (2008), the 'post-peak decrease' curves like Festulolium grass in this study are usually found in root systems possessing many fine roots spread over the failure plane, causing failure in the manner of a composite root-soil matrix with high reinforcement rather than by root anchorage mechanisms. This fits with the measured RAR distribution in terms of root diameter shown in Fig. 14. For most shear planes, Willow and Gorse roots thicker than 0.5 mm contributed at least 50% of the RAR, whilst Festulolium grass roots finer than 0.5 mm contributed the bulk of RAR. During shearing, the progressive post-peak decrease in shear resistance for Festulolium grass was probably due to the progressive breakage of those fine roots in which the tensile strength was fully mobilized (Loades et al., 2010; Comino et al., 2010). This may also explain why a relatively higher root soil interaction factor k was observed for Festulolium grass (see Eq. (4)). For Willow and Gorse, many roots were probably yet to mobilize their full tensile strength; as a result, they continued to confer resistance to shear and no post peak reduction of shear resistance was observed (Docker and Hubble, 2008).

Root contribution to shear strength in the field can be obtained in one of three ways: (i) Analytical calculation based on root properties, e.g. use of WWM (Wu, 1976; Waldron, 1977) or FBM (Pollen and Simon, 2005); (ii) In-situ/laboratory shear testing; (iii) Back–calculation from observed slope failures. The derived additional shear strength value based on measured root strengths from tensile tests in (i) does not include the mechanical function of large structural roots (larger than 10–20 mm in diameter) which tend to bend or rotate, rather than breaking in tension; the applicability of such models for thin roots still requires further validation given reported over-predication in previous studies (e.g. Docker and Hubble, 2008; Loades et al., 2010; Sonnenberg et al., 2011). Back calculated shear strength increases from slope stability models generally assume rooted soil is a homogenous material with cohesion uniformly distributed over the entire slope profile at the shear surface. This can lead to overprediction of stability and underprediction of root contribution (Liang et al., 2015). Direct shear tests are generally performed on young plants and/or on very shallow shear plane (less than 0.2 m) due to limitations of available shear apparatus, but can be considered more reliable compared to (i) and (iii). Table 6 presents a collection of in situ direct shear studies on mature rooted soil since 1996. Compared with the data before 1996 collected by Schmidt et al. (2001) and Wu (2013), no significant difference was observed, values generally are around several kPa and seldom higher than 20 kPa. Noticeably stronger values were reported by Fan and Chen (2010) where tests were performed on much older trees.

Fig. 18 shows a comparison of increased shear strength in this study (at an indicative scale $N = 15$) with the in situ shear tests data on young trees in Table 6 and derived mature tree data reported by Docker and Hubble (2009). Here the shear strength increase was directly taken from the measured values, which represent the lower bound values considering the effect of soil confining stress on the shear strength increase of rooted soil (Duckett, 2013; Liang et al., 2017). The study by Docker and Hubble (2009) is highlighted here because (i) it considered root reinforcement within the soil deeper than 1 m, and (ii) considered the lateral variation of root reinforcement, as shown in the form of two lines for each species in Fig. 18. Here the upper bound line represents the increased shear strength within the zone of rapid taper of the tree (Danjon and Reubens, 2008), with the lower bound line representing the shear strength increase within the first layer outside the zone of rapid taper. The shear strength increases measured in our study at prototype scale represents an upper bound of young trees compared with the direct shear tests, but a lower bound for field mature trees.

4.4. Selection of a suitable scaling factor for centrifuge modelling

To benefit most from using the centrifuge modelling technique to model a prototype slope of larger height at small scale (1:N), without generating unwanted boundary effects from the model container, it is desirable to select a high value of N. However, as suggested by Kutter (1995) and Taylor (2003), for modelling of reinforced slopes, if a structure (e.g. a fine root in this study) is relatively small compared to the median size of the soil particles (D_{50}), then the soil may no longer behave as a continuum but more as a set of discrete particles. Therefore, to minimise potential grain size effects on the root-soil interaction, the lowest possible N is preferred. In this study, the Bullionfield soil used contained 10% very fine (clay; Fig. 1) particles, together with a larger proportion of silt. These fine particles may occupy many of the voids between the larger sand particles. Considering the ratio between the root diameters and the fine particles is relatively large (>50), the particle size effect is considered to be non-significant here. Furthermore, there are limits on working durations of centrifuges based on the time scaling law in Table 1. For example, to model 1 year of prototype time will take 3.65 days of continuous spanning to achieve this at a scale of 1:10; hence, selection of a high value of N is again preferred. Finally, for

Please cite this article in press as: Liang, T., et al., Scaling of the reinforcement of soil slopes by living plants in a geotechnical centrifuge. Ecol. Eng. (2017), http://dx.doi.org/10.1016/j.ecoleng.2017.06.067

Table 6
Data collected from recent studies (since 1996) on shear strength increase due to the presence of roots measured from in-situ shear test.

No	species	site	plant type	soil	Shear depth (m)	Fallow Soil strength (kPa)	Shear strength increase (kPa)	Shear strength increase ratio (%)	RAR (%)
1	*C. glauca*	Nepean River, Australia	Tree	brown loams and sandy loams	0.29	20.10	6.9	34	0.143
2	*E. amplifolia*	Nepean River, Australia	Tree	brown loams and sandy loams	0.29	17.64	8.9	50	0.211
3	*E. elata*	Nepean River, Australia	Tree	brown loams and sandy loams	0.29	17.02	10.58	62	(0.02–0.73) 0.221
4	*A. floribunda*	Nepean River, Australia	Tree	brown loams and sandy loams	0.29	14.55	17.79	122	(0.01–0.23) 0.082
5	*Linden hibiscus*	Kaohsiung City, Taiwan	Tree	sandy and clayey soils	0.1	9.52	5.32–20.21	56–212	0.57–4.25
6	*Japanese Mallotus*	Kaohsiung City, Taiwan	Tree	sandy and clayey soils	0.1	9.52	12.77–32.98	134–346	0.64–3.19
7	*Chinese tallow tree*	Kaohsiung City, Taiwan	Tree	sandy and clayey soils	0.1	9.52	15.37–57.24	161–601	1.6–7.6
8	*ironwood*	Kaohsiung City, Taiwan	Tree	sandy and clayey soils	0.1	9.52	23.49–72.60	247–763	1.1–4.2
9	*white popinac*	Kaohsiung City, Taiwan	Tree	sandy and clayey soils	0.1	9.52	14.36–70.21	151–741	1.7–9.5
10	*Pinus pinaster*	A ravine (barranco)	Tree	calcaric cambisols	0.4	1.9–10.2	3.3–18.2	55–301	/
11	*Pinus radiata*	New Zealand	Tree	SM	0.5	7	2.5–4.5	36–64	/
12	*Pinus radiata*	New Zealand	Tree	Silty clay	0.15	13.3–17.3	10.6–18.9	69.3–124	/
13	Kanuka	New Zealand	Tree	Silty clay	0.15	10.2–16.4	5.85–23.15	43.8–173	/
14	*Pinus halepensis*	SE Spain	Tree	Colluvial and residual soils	0.4	4.1–10.2	5.9 ± 7.5	82.5	/
15	*Sesbania cannabina* Merr.	Kaohsiung City, Taiwan	Shrub	sands mixed with silts and clay	0.1	9.52	0.5–20.18	5–212	0.15–0.45
16	*Vetiveria zizanioides*	Almudaina, Spain	Grass	silt with a high clay content	0.2	4.4–5.9	2.1–3.7	12–55	0.034–0.071
17	*Lotus corniculatus*	Italian Alpine	Grass	SM/SW	0.1	1.5 ± 0.9	10.2 ± 3.4	693	0.102 ± 0.078
18	*Trifolium pratense*	Italian Alpine	Grass	SM/SW	0.1	1.5 ± 0.9	7.6 ± 2.8	515	0.033 ± 0.017
19	*Medicago sativa*	Italian Alpine	Grass	SM/SW	0.1	1.5 ± 0.9	7.8 ± 2.3	530	0.069 ± 0.026
20	*Festuca pratensis*	Italian Alpine	Grass	SM/SW	0.1	5.5 ± 2.9	8.9 ± 1.9	161	0.059 ± 0.023
21	*Lolium perenne*	Italian Alpine	Grass	SM/SW	0.1	5.5 ± 2.9	8.6 ± 2.3	154	0.060 ± 0.040
22	*Vetiver Ziznoides (L.) Nash*	Thailand	Grass	clay	0.1	8.77–9.58	2.3–8.0	24–91	/
23	*Brachiaria Ruziziensis*	Thailand	Grass	clay	0.1	8.77–9.58	1.2–2.0	13–23	/
24	*herbaceous cover*	A ravine (barranco)	Grass	calcaric cambisols	0.4	1.9–10.2	0.5–0.7	8–12	/
25	*Vetiveria zizanioides*	Malaysia	Grass	/	0.25	9.89	8.92	90.2	0.0331
					0.50	10.61	4.17	39.3	0.0176
					0.75	10	3.46	34.6	0.0138
					1.0	9.92	2.61	26.3	0.0107
					1.25	10.21	1.94	19.0	0.0071
					1.50	10.24	1.28	12.5	0.0052
26	*Brachypodium distachyon* L. Beauv *and others*	SE Spain	Grass	Colluvial and residual soils	0.4	4.1–10.2	0.6 ± 0.1	8.39	/

Data Source: 1–4: Docker and Hubble, (2008); 5–9: Fan and Chen (2010); 10: Van Beek et al. (2005); 11: Wu and Watson (1998); 12–13: Ekanayake et al. (1998); 14: Cammeraat et al. (2005); 15: Fan and Su (2008); 16: Mickovski and Van Beek (2009); 17–21: Comino et al. (2010); Comino and Druetta (2010); 22–23: Teerawattanasuk et al. (2014) 24: Van Beek et al. (2005); 25: Hengchaovanich and Nilaweera (1996); 26: Cammeraat et al. (2005).

Please cite this article in press as: Liang, T., et al., Scaling of the reinforcement of soil slopes by living plants in a geotechnical centrifuge. Ecol. Eng. (2017), http://dx.doi.org/10.1016/j.ecoleng.2017.06.067

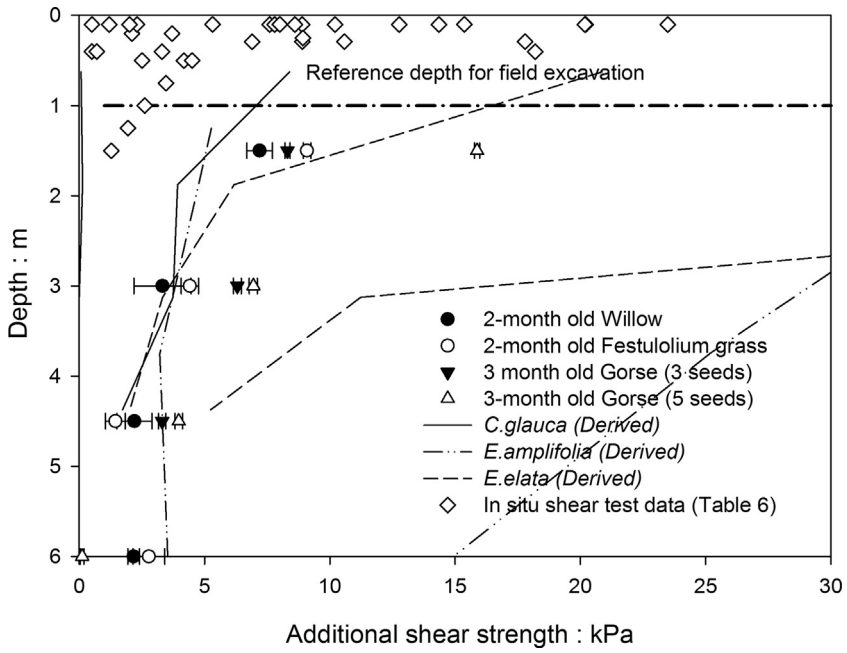

Fig. 18. Comparison between the increased shear strength provided by the juvenile plants cultivated in this study at prototype scale (note: rooting depth is scaled up by an indicative scale of $N = 15$ with root reinforcement scaled 1:1, see Table 1) and root reinforcement data collected from the literature.

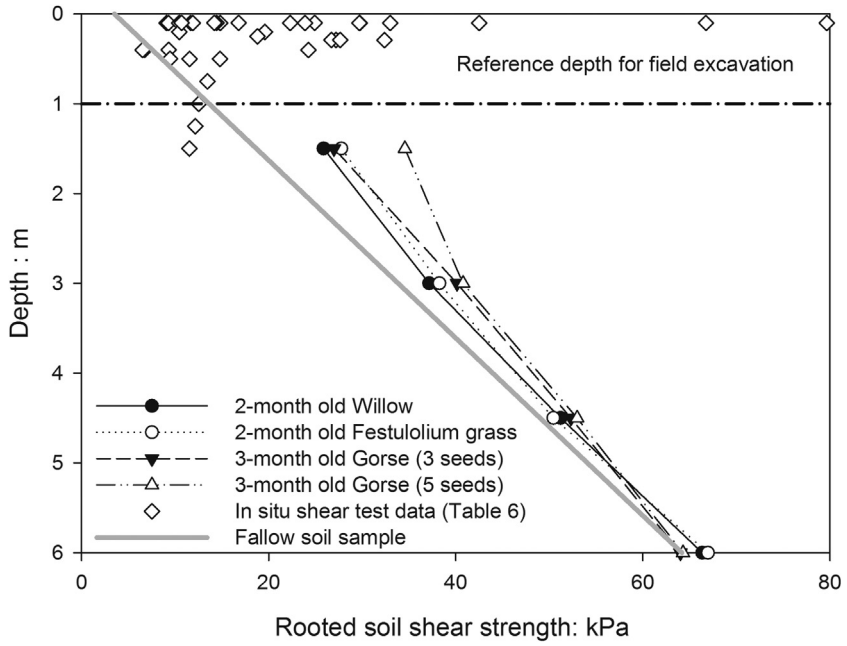

Fig. 19. Comparison between the soil shear strength planted with the juvenile plants cultivated in this study at prototype scale (note: rooting depth is scaled up by an indicative scale of N = 15 with root reinforcement scaled 1:1, see Table 1) between field rooted soil strength collected from the literature.

a rooted slope problem a high value of N implies a deeper rooting depth at prototype scale, which is not preferred for modelling the rooted slope response given rooting depths observed in the field for mature plants. A scale of 1:15 ($N = 15$) was ultimately decided upon as a suitable compromise for model testing using the species considered in this study given these competing effects.

If model rooting depth (450 mm) is scaled up by 15 times, the root depth at prototype scale would be 6.75 m. Such values, however, can be considered in the same order of magnitude with the global maximum rooting depth of trees and shrubs, but too deep for herbaceous plants (2.6 ± 0.1 m). Much shallower rooting depths would be required when modelling herbaceous plants. Additional tests have been conducted for Festulolium grass in 50 mm diameter tubes under the same growing conditions as this study to investigate the change of rooting depth with time. It was found that grass root depth extended to 174 ± 50.1 mm and 450 ± 0 mm after 2 weeks and 4 weeks of growing, respectively. However, these young roots were relatively weak, which had low mechanical strength (hence low additional shear strength). From a centrifuge modelling perspective, a compromise would have to be made to resolve the conflicts between rooting depth and root mechanical properties if herbaceous plants are to be modelled.

In addition to considering the magnitude of soil strength increase due to the presence of roots (Fig. 18), the increase in soil

Please cite this article in press as: Liang, T., et al., Scaling of the reinforcement of soil slopes by living plants in a geotechnical centrifuge. Ecol. Eng. (2017), http://dx.doi.org/10.1016/j.ecoleng.2017.06.067

strength with depth relative to the strength of fallow soil at prototype scale in the centrifuge is shown in Fig. 19. The soil strength increases in the deeper soil layers (>3 m) are negligible compared with the fallow soil strength at the same depth (less than 30% increase). Hence, when the plants are tested in a geotechnical centrifuge, the most significant contributions of roots to soil strength are mainly located in the shallow soil layer, which is typical of field cases based on the available data. For modelling root reinforced slopes, centrifuge modelling using juvenile plant roots may not be perfect, but it can still provide a representative and informative mechanical model.

5. Conclusion

For modelling of slope stability problems at small scale in a geotechnical centrifuge, use of juvenile plants could potentially produce prototype root systems that are highly representative of corresponding mature root systems both in terms of root mechanical properties and root morphology when a suitable growing time and scaling factor for the slope model are selected. The three selected species of willow, gorse and grass developed distinct root morphologies, and root-soil interaction (root-soil interaction k values of 0.367, 1.12 and 0.325 for Willow, Festulolium grass and Gorse, respectively) when subject to shear loading and were identified to be a good choice for centrifuge modelling to represent distinct plant groups. However, it remains a substantial challenge to simultaneously capture the distribution of root biomass with depth of the corresponding mature plant. Therefore, a compromise has to be made to resolve the conflicts between the scaling of rooting depth in terms of the presence of root biomass and depth of root reinforcement in terms of the effect on shear strength. Based on the test results and also the consideration of various physical constraints in centrifuge modelling, a scale of 1:15 appears a suitable compromise for correct model scaling and testing of the three selected species. Our results show that the age of plants affects the choice of the scaling factor: Two-month old juvenile plants appear a good choice for scaling of root reinforced slopes using live plants at 1:15 scale. Using plants older than 2 months (such as the 3-month old Gorse considered) may lead to a prototype with root biomechanical properties which are overly strong and stiff, and hence potentially unrepresentative of root-soil interaction during slippage.

Apart from the main findings, our test results also show that when all juvenile root samples of the three species are considered, the commonly used negative power law does not fit the data for the relationship between root tensile strength and root diameter well, resulting in very low R^2 values. However, a strong linear relationship was observed between root tensile strength and root Young's modulus of the juvenile plants. Although such correlation is not certain for mature plants, this highly correlated relationship would facilitate future interpretation of root failure mechanism and reinforcement in centrifuge model slopes as well as numerical modelling of soil-root mechanical interaction.

Acknowledgements

The research described here in was funded by a EPSRC (EP/M020355/1) project in collaboration with the University of Dundee, the University of Southampton, the University of Aberdeen, the Durham University and The James Hutton Institute. The authors thank Professor Mike Humphreys (IBERS, Aberystwyth University) and Scotia seeds for providing seeds used in this study and Dr Gary Callon (University of Dundee) for arranging indoor growing area. The James Hutton Institute receives funding from the Scottish Government (Rural & Environmental Services & Analytical Services Division).

References

Adhikari, A.R., Gautam, M.R., Yu, Z., Imada, S., Acharya, K., 2013. Estimation of root cohesion for desert shrub species in the Lower Colorado riparian ecosystem and its potential for streambank stabilization. Ecol. Eng. 51, 33–44, http://dx.doi.org/10.1016/j.ecoleng.2012.12.005.

Askarinejad, A., Springman, S.M., 2015. Centrifuge modelling of the effects of vegetation on the response of a silty sand slope subjected to rainfall. In: Computer Methods and Recent Advances in Geomechanics. Taylor & Francis Group, London, UK, pp. 1339–1344.

Bengough, A.G., Loades, K., McKenzie, B.M., 2016. Root hairs aid soil penetration by anchoring the root surface to pore walls. J. Exp. Bot. 67, 1071–1078, http://dx.doi.org/10.1093/jxb/erv560.

Bischetti, G.B., Chiaradia, E.A., Simonato, T., Speziali, B., Vitali, B., Vullo, P., Zocco, A., 2005. Root strength and root area ratio of forest species in lombardy (Northern Italy). Plant Soil 278, 11–22, http://dx.doi.org/10.1007/s11104-005-0605-4.

Bischetti, G.B., Chiaradia, E.A., Epis, T., Morlotti, E., 2009. Root cohesion of forest species in the Italian Alps. Plant Soil 324, 71–89, http://dx.doi.org/10.1007/s11104-009-9941-0.

Boldrin, D., Leung, A.K., Bengough, A.G., 2017a. Correlating hydrologic reinforcement of vegetated soil with plant traits during establishment of woody perennials. Plant Soil, 1–15, http://dx.doi.org/10.1007/s11104-017-3211-3.

Boldrin, D., Leung, A.K., Bengough, A.G., 2017b. Root biomechanical properties during establishment of woody perennials. Ecol. Eng., http://dx.doi.org/10.1016/j.ecoleng.2017.05.002, in press G Model.

Cammeraat, E., Van Beek, R., Kooijman, A., 2005. Vegetation succession and its consequences for slope stability in SE Spain. Plant Soil 278, 135–147, http://dx.doi.org/10.1007/s11104-005-5893-1.

Canadell, J., Jackson, R.B., Ehleringer, J.B., Mooney, H. a., Sala, O.E., Schulze, E.-D., 1996. Maximum rooting depth of vegetation types at the global scale. Oecologia 108, 583–595, http://dx.doi.org/10.1007/BF00329030.

Comino, E., Druetta, A., 2010. The effect of Poaceae roots on the shear strength of soils in the Italian alpine environment. Soil Tillage Res. 106, 194–201, http://dx.doi.org/10.1016/j.still.2009.11.006.

Comino, E., Marengo, P., Rolli, V., 2010. Root reinforcement effect of different grass species: a comparison between experimental and models results. Soil Tillage Res. 110, 60–68, http://dx.doi.org/10.1016/j.still.2010.06.006.

Danjon, F., Reubens, B., 2008. Assessing and analyzing 3D architecture of woody root systems, a review of methods and applications in tree and soil stability, resource acquisition and allocation. Plant Soil 303, 1–34, http://dx.doi.org/10.1007/s11104-007-9470-7.

Davies, M.C.R., Bowman, E.T., White, D.J., 2010. Physical modelling of natural hazards. In: Physical Modelling in Geotechnics, Two Volume Set: Proceedings of the 7th International Conference on Physical Modelling in Geotechnics (ICPMG 2010), 28th June–1st July CRC Press Zurich, Switzerland, pp. 3–22.

Docker, B.B., Hubble, T.C.T., 2008. Quantifying root-reinforcement of river bank soils by four Australian tree species. Geomorphology 100, 401–418, http://dx.doi.org/10.1016/j.geomorph.2008.01.009.

Docker, B.B., Hubble, T.C.T., 2009. Modelling the distribution of enhanced soil shear strength beneath riparian trees of south-eastern Australia. Ecol. Eng. 35, 921–934, http://dx.doi.org/10.1016/j.ecoleng.2008.12.018.

Duckett, N., 2013. Development of Improved Predictive Tools for Mechanical Soil-Root Interaction. PhD Thesis. University of Dundee, UK.

Eab, K., Takahashi, A., Likitlersuang, S., 2014. Centrifuge modelling of root-reinforced soil slope subjected to rainfall infiltration. Géotech. Lett. 4, 211–216, http://dx.doi.org/10.1680/geolett.14.00029.

Ekanayake, J., Marden, M., Watson, A., Rowan, D., 1998. Tree-roots and slope stability: a comparison between Pinus radiata and Kanuka. N. Z. J. For. Sci. 27, 216–233.

Fan, C.C., Chen, Y.W., 2010. The effect of root architecture on the shearing resistance of root-permeated soils. Ecol. Eng. 36, 813–826, http://dx.doi.org/10.1016/j.ecoleng.2010.03.003.

Fan, C.C., Su, C.F., 2008. Role of roots in the shear strength of root-reinforced soils with high moisture content. Ecol. Eng. 33, 157–166, http://dx.doi.org/10.1016/j.ecoleng.2008.02.013.

Genet, M., Stokes, A., Salin, F., Mickovski, S.B., Fourcaud, T., Dumail, J.F., Van Beek, R., 2005. The influence of cellulose content on tensile strength in tree roots. Plant Soil 278, 1–9, http://dx.doi.org/10.1007/s11104-005-8768-6.

Ghestem, M., Cao, K., Ma, W., Rowe, N., Leclerc, R., Gadenne, C., Stokes, A., 2014a. A framework for identifying plant species to be used as ecological engineers for fixing soil on unstable slopes. PLoS One 9, http://dx.doi.org/10.1371/journal.pone.0095876.

Ghestem, M., Veylon, G., Bernard, A., Vanel, Q., Stokes, A., 2014b. Influence of plant root system morphology and architectural traits on soil shear resistance. Plant Soil 377, 43–61, http://dx.doi.org/10.1007/s11104-012-1572-1.

Hales, T.C., Ford, C.R., Hwang, T., Vose, J.M., Band, L.E., 2009. Topographic and ecologic controls on root reinforcement. J. Geophys. Res. Solid Earth 114, http://dx.doi.org/10.1029/2008jf001168.

Hengchaovanich, D., Nilaweera, N.S., 1996. An assessment of strength properties of vetiver grass roots in relation to slope stabilisation. In: Proceeding of First

International Vetiver Conference, Chain Kai, Thailand, Office of the Royal Development Projects Board, Bangkok, Thailand, pp. 153–158.
Hinsinger, P., Bengough, A.G., Vetterlein, D., Young, I.M., 2009. Rhizosphere: biophysics, biogeochemistry and ecological relevance. Plant Soil 321, 117–152, http://dx.doi.org/10.1007/s11104-008-9885-9.
Jackson, R.B., Canadell, J., Ehleringer, J.R., Mooney, H. a., Sala, O.E., Schulze, E.D., 1996. A global analysis of root distributions for terrestrial biomes. Oecologia 108, 389–411, http://dx.doi.org/10.1007/BF00333714.
Kim, J.H., Fourcaud, T., Jourdan, C., Maeght, J.-L., Mao, Z., Metayer, J., Meylan, L., Pierret, A., Rapidel, B., Roupsard, O., de Rouw, A., Sanchez, M.V., Wang, Y., Stokes, A., 2017. Vegetation as a driver of temporal variations in slope stability: the impact of hydrological processes. Geophys. Res. Lett., 1–11, http://dx.doi.org/10.1002/2017GL073174.
Kutter, B., 1995. Recent advances in centrifuge modeling of seismic shaking. In: Proceedings of the Third International Conference on Recent Advances in Geotechnical Earthquake Engineering and Soil Dynamics, St. Louis, Missouri, pp. 927–941.
Liang, T., Knappett, J.A., 2017. Centrifuge modelling of the influence of slope height on the seismic performance of rooted slopes. Geotechnique, http://dx.doi.org/10.1680/jgeot.16.p.072.
Liang, T., Knappett, J.A., Bengough, A.G., 2014. Scale modelling of plant root systems using 3-D printing. In: Proceedings of the 8th International Conference on Physical Modelling in Geotechnics, Perth, Australia, Thomas Telford, pp. 361–366.
Liang, T., Knappett, J.A., Duckett, N., 2015. Modelling the seismic performance of rooted slopes from individual root–soil interaction to global slope behaviour. Géotechnique 65, 995–1009, http://dx.doi.org/10.1680/jgeot.14.P.207.
Liang, T., Knappett, J.A., Bengough, A.G., Ke, Y.X., 2017. Small scale modelling of plant root systems using 3-D printing, with applications to investigate the role of vegetation on earthquake induced landslides. Landslides, http://dx.doi.org/10.1007/s10346-017-0802-2.
Loades, K.W., Bengough, A.G., Bransby, M.F., Hallett, P.D., 2010. Planting density influence on fibrous root reinforcement of soils. Ecol. Eng. 36, 276–284, http://dx.doi.org/10.1016/j.ecoleng.2009.02.005.
Loades, K.W., Bengough, A.G., Bransby, M.F., Hallett, P.D., 2013. Biomechanics of nodal, seminal and lateral roots of barley: effects of diameter, waterlogging and mechanical impedance. Plant Soil 370, 407–418, http://dx.doi.org/10.1007/s11104-013-1643-y.
Loades, K.W., Bengough, A.G., Bransby, M.F., Hallett, P.D., 2015. Effect of root age on the biomechanics of seminal and nodal roots of barley (Hordeum vulgare L.) in contrasting soil environments. Plant Soil 395, 253–261, http://dx.doi.org/10.1007/s11104-015-2560-z.
Macleod, C.K.J.A., Humphreys, M.W., Whalley, W.R., Turner, L., Binley, A., Watts, C.W., Skøt, L., Joynes, A., Hawkins, S., King, I.P., O'Donovan, S., Haygarth, P.M., 2013. A novel grass hybrid to reduce flood generation in temperate regions. Sci. Rep. 3, 1683, http://dx.doi.org/10.1038/srep01683.
Mao, Z., Saint-André, L., Genet, M., Mine, F.X., Jourdan, C., Rey, H., Courbaud, B., Stokes, A., 2012. Engineering ecological protection against landslides in diverse mountain forests: choosing cohesion models. Ecol. Eng. 45, 55–69, http://dx.doi.org/10.1016/j.ecoleng.2011.03.026.
Mattia, C., Bischetti, G.B., Gentile, F., 2005. Biotechnical characteristics of root systems of typical Mediterranean species. Plant Soil 278, 23–32, http://dx.doi.org/10.1007/s11104-005-7930-5.
Meijer, G.J., Bengough, A.G., Knappett, J.A., Loades, K.W., Nicoll, B.C., 2016. New in situ techniques for measuring the properties of root-reinforced soil −laboratory evaluation. Geotechnique 66, 27–40, http://dx.doi.org/10.1680/jgeot.15.P.060.
Meijer, G.J., 2016. New Methods for in Situ Measurement of Mechanical Root-Reinforcement on Slopes. PhD Thesis. University of Dundee, UK.
Mickovski, S.B., Van Beek, L.P.H., 2009. Root morphology and effects on soil reinforcement and slope stability of young vetiver (Vetiveria zizanioides) plants grown in semi-arid climate. Plant Soil 324, 43–56, http://dx.doi.org/10.1007/s11104-009-0130-y.
Mickovski, S.B., Bengough, A.G., Bransby, M.F., Davies, M.C.R., Hallett, P.D., Sonnenberg, R., 2007. Material stiffness, branching pattern and soil matric potential affect the pullout resistance of model root systems. Eur. J. Soil Sci. 58, 1471–1481, http://dx.doi.org/10.1111/j.1365-2389.2007.00953.x.
Mickovski, S.B., Hallett, P.D., Bransby, M.F., Davies, M.C.R., Sonnenberg, R., Bengough, A.G., 2009. Mechanical reinforcement of soil by willow roots: impacts of root properties and root failure mechanism. Soil Sci. Soc. Am. J. 73, 1276–1285, http://dx.doi.org/10.2136/sssaj2008.0172.
Muir Wood, D., 2003. Geotechnical Modelling. CRC Press.
Ng, C.W.W., Leung, A.K., Kamchoom, V., Garg, A., 2014. A novel root system for simulating transpiration-induced soil suction in centrifuge. Geotech. Test. J. 37, 1–16, http://dx.doi.org/10.1520/GTJ20130116.
Ng, C.W.W., Kamchoom, V., Leung, A.K., 2016. Centrifuge modelling of the effects of root geometry on transpiration-induced suction and stability of vegetated slopes. Landslides 13, 925–938, http://dx.doi.org/10.1007/s10346-015-0645-7.
Normaniza, O., Faisal, H.A., Barakbah, S.S., 2008. Engineering properties of Leucaena leucocephala for prevention of slope failure. Ecol. Eng. 32, 215–221, http://dx.doi.org/10.1016/j.ecoleng.2007.11.004.
Operstein, V., Frydman, S., 2000. The influence of vegetation on soil strength. Proc. Ice-Gr. Improv. 4, 81–89.
Pollen, N., Simon, A., 2005. Estimating the mechanical effects of riparian vegetation on stream bank stability using a fiber bundle model. Water Resour. Res. 41, 1–11, http://dx.doi.org/10.1029/2004WR003801.
Pollen, N., 2007. Temporal and spatial variability in root reinforcement of streambanks: accounting for soil shear strength and moisture. Catena 69, 197–205, http://dx.doi.org/10.1016/j.catena.2006.05.004.
Schmidt, K.M., Roering, J.J., Stock, J.D., Dietrich, W.E., Montgomery, D.R., Schaub, T., 2001. The variability of root cohesion as an influence on coast range. Can. Geotech. J. 38, 995–1024, http://dx.doi.org/10.1139/cgj-38-5-995.
Schmidt, S., Gregory, P.J., Grinev, D.V., Bengough, A.G., 2013. Root elongation rate is correlated with the length of the bare root apex of maize and lupin roots despite contrasting responses of root growth to compact and dry soils. Plant Soil 372, 609–618, http://dx.doi.org/10.1007/s11104-013-1766-1.
Schofield, A., 1981. Dynamic and earthquake geotechnical centrifuge modelling. In: Proceeding of International Conference on Recent Advances in Geotechnical Earthquake Engineering and Soil Dynamics, University of Missouri-Rolla, pp. 1081–1100.
Schwarz, M., Cohen, D., Or, D., 2010a. Root-soil mechanical interactions during pullout and failure of root bundles. J. Geophys. Res. Earth Surf. 115, F04035, http://dx.doi.org/10.1029/2009JF001603.
Schwarz, M., Lehmann, P., Or, D., 2010b. Quantifying lateral root reinforcement in steep slopes – from a bundle of roots to tree stands. Earth Surf. Process. Landforms 35, 354–367, http://dx.doi.org/10.1002/esp.1927.
Schwarz, M., Preti, F., Giadrossich, F., Lehmann, P., Or, D., 2010c. Quantifying the role of vegetation in slope stability: a case study in Tuscany (Italy). Ecol. Eng. 36, 285–291, http://dx.doi.org/10.1016/j.ecoleng.2009.06.014.
Simon, A., Collison, A.J.C., 2002. Quantifying the mechanical and hydrologic effects of riparian vegetation on streambank stability. Earth Surf. Process. Landforms 27, 527–546, http://dx.doi.org/10.1002/esp.325.
Smethurst, J., Clarke, D., Powrie, W., 2006. Seasonal changes in pore water pressure in a grass covered cut slope in London clay. Geotechnique 56, 523–537, http://dx.doi.org/10.1680/geot.2006.56.8.523.
Smethurst, J., Clarke, D., Powrie, W., 2012. Factors controlling the seasonal variation in soil water content and pore water pressures within a lightly vegetated clay slope. Geotechnique 62, 429–446.
Smethurst, J.A., Briggs, K.M., Powrie, W., Ridley, A., Butcher, D.J.E., 2015. Mechanical and hydrological impacts of tree removal on a clay fill railway embankment. Geotechnique 65, 869–882.
Sonnenberg, R., Bransby, M.F., Hallett, P.D., Bengough, A.G., Mickovski, S.B., Davies, M.C.R., 2010. Centrifuge modelling of soil slopes reinforced with vegetation. Can. Geotech. J. 47, 1415–1430, http://dx.doi.org/10.1139/T10-037.
Sonnenberg, R., Bransby, M.F., Bengough, A.G., Hallett, P.D., Davies, M.C.R., 2011. Centrifuge modelling of soil slopes containing model plant roots. Can. Geotech. J. 49, 1–17, http://dx.doi.org/10.1139/T11-081.
Stokes, A., Atger, C., Bengough, A.G., Fourcaud, T., Sidle, R.C., 2009. Desirable Plant root traits for protecting natural and engineered slopes against landslides. Plant Soil 324, 1–30, http://dx.doi.org/10.1007/s11104-009-0159-y.
Stokes, A., Douglas, G.B., Fourcaud, T., Giadrossich, F., Gillies, C., Hubble, T., Kim, J.H., Loades, K.W., Mao, Z., McIvor, I.R., Mickovski, S.B., Mitchell, S., Osman, N., Phillips, C., Poesen, J., Polster, D., Preti, F., Raymond, P., Rey, F., Schwarz, M., Walker, L.R., 2014. Ecological mitigation of hillslope instability: ten key issues facing researchers and practitioners. Plant Soil 377, 1–23, http://dx.doi.org/10.1007/s11104-014-2044-6.
Take, W.A., Bolton, M.D., 2011. Seasonal ratcheting and softening in clay slopes, leading to first-time failure. Géotechnique 61, 757–769, http://dx.doi.org/10.1680/geot.9.P.125.
Taylor, R.N., 2003. Geotechnical Centrifuge Technology. CRC Press.
Teerawattanasuk, C., Maneecharoen, J., Bergado, D.T., Voottipruex, P., Lam, L.G., 2014. Root strength measurements of Vetiver and Ruzi grasses. Lowl. Technol. Int. 16, 71–80.
Van Beek, L.P.H., Wint, J., Cammeraat, L.H., Edwards, J.P., 2005. Observation and simulation of root reinforcement on abandoned mediterranean slopes. Plant Soil 278, 55–74, http://dx.doi.org/10.1007/s11104-005-7247-4.
Veylon, G., Ghestem, M., Stokes, A., Bernard, A., 2015. Quantification of mechanical and hydric components of soil reinforcement by plant roots. Can. Geotech. J. 11, 1–11, http://dx.doi.org/10.1139/cgj-2014-0090.
Waldron, L.J., 1977. The shear resistance of root-permeated homogeneous and stratified soil. Soil Sci. Soc. Am. J. 41, 843–849, http://dx.doi.org/10.2136/sssaj1977.03615995004100050005x.
Wu, T.H., Watson, A., 1998. In situ shear tests of soil blocks with roots. Can. Geotech. J. 35, 579–590, http://dx.doi.org/10.1139/t98-e027.
Wu, T., Kokesh, Christopher M., Trenner, B.R., Fox, P.J., 2014. Use of live poles for stabilization of a shallow slope failure. J. Geotech. Geoenviron. Eng. 140, 1–13, http://dx.doi.org/10.1061/(ASCE)GT.1943-5606.0001161.
Wu, T.H., 1976. Investigation of landslides on Prince of Wales Island, Alaska. Geotech. Eng. Rep., 5. Civ. Eng. Dep. Ohio State Univ., Columbus, Ohio, USA.
Wu, T.H., 2013. Root reinforcement of soil: review of analytical models, test results, and applications to design. Can. Geotech. J. 50, 259–274.
Zhang, C.B., Chen, L.H., Jiang, J., 2014. Why fine tree roots are stronger than thicker roots: the role of cellulose and lignin in relation to slope stability. Geomorphology 206, 196–202, http://dx.doi.org/10.1016/j.geomorph.2013.09.024.
van Genuchten, M.T., 1980. A closed-form equation for predicting the hydraulic conductivity of unsaturated soils1. Soil Sci. Soc. Am. J. 44, 892, http://dx.doi.org/10.2136/sssaj1980.03615995004400050002x.

Please cite this article in press as: Liang, T., et al., Scaling of the reinforcement of soil slopes by living plants in a geotechnical centrifuge. Ecol. Eng. (2017), http://dx.doi.org/10.1016/j.ecoleng.2017.06.067